



Stockholm
University

Master Thesis

Degree Project in
Geochemistry 15 hp

Using Ni isotopes as biosignatures

Arjen Boosman

Stockholm 2016

Department of Geological Sciences
Stockholm University
SE-106 91 Stockholm

Nickel isotopes as a biomarker

a non-traditional isotope system as an indicator for biotic methanogenesis

Guided Research, 30ECTS

A. J. Boosman

Master Earth Structure and Dynamics

Departement Aardwetenschappen, Universiteit Utrecht, Utrecht, The Netherlands

3899101, a.j.boosman@students.uu.nl

Performed at Stockholm University, Stockholm, Sweden and

L'Institut Français de Recherche pour l'Exploitation de la Mer, Brest, France

June 2016

Abstract

Nickel (Ni) is a key element in metabolic pathways of methanogenic Archaea due to its use in Ni-enzymes. Ni is strongly fractionated during its absorption by methanogens. $\Delta^{60}\text{Ni}$ values ($\delta^{60}\text{Ni}_{\text{cell}} - \delta^{60}\text{Ni}_{\text{environment}}$) as low as -2‰ have been reported in methanogenic cultures. However, Ni sorption to particles, e.g. clays and Fe oxides, and organic ligands can yield similar fractionation patterns. The usefulness of Ni as a biomarker has been proposed and debated. Cell culture experiments confirm general negative $\Delta^{60}\text{Ni}$ values on the order of 1 to 2‰. In some cases cells do not display the well known negative $\Delta^{60}\text{Ni}$ signature, most likely due to simultaneous abiotic fractionation by organic ligands. Experiments suggest increasing fractionation with increased Ni concentrations in growth media. To assess Ni as a viable biomarker for methanogens, we provide new Ni isotope data from rocks and fluids from an outcrop of the Tekirova ophiolite, Turkey, a system undergoing serpentinization with active CH_4 and fluid seeps. Methanogen presence and hence a partially biogenic origin of the CH_4 are confirmed. In one locality, methanogen presence can be linked to a negative excursion in $\delta^{13}\text{C}$ and a significantly lower $\delta^{60}\text{Ni}$ value. There is no mineralogical explanation for the negative $\delta^{60}\text{Ni}$ excursion, hence we suggest that the fractionation of Ni may be a true Ni biosignature. The viability of Ni as a biomarker for extraterrestrial or early terrestrial life is doubtful, due to the large number of Ni fractionating processes and our limited understanding of the Ni budget in e.g. the oceans and the biosphere. Future research should focus on revealing abiotic fractionation in relevant processes, such as serpentinization and the formation of BIFs and on in-situ analysis of Ni isotopes of microfossils.

First Supervisor:

dr. Paul Mason

Department of Earth Sciences

Universiteit Utrecht

p.mason@uu.nl

Second Supervisor:

dr. Anna Neubeck

Institute for Geological Sciences

Stockholm University

Table of contents	1
<hr/>	
Introduction	2
<hr/>	
Background: Nickel and methanogenesis in nature	3
Ni isotopes	3
Ni isotopes throughout the Earth	3
Abiotic Ni fractionation	3
Biotic methanogenesis and Ni fractionation	4
Oceanic Ni across the GOE	4
Methanogenesis on Earth through serpentinization	4
Geology of the Tekirova ophiolite	6
<hr/>	
Materials and Methods	7
Sample description	7
X-ray diffraction	8
Mass bias, interference, and the ^{61}Ni - ^{62}Ni double spike	9
Ni elution through liquid column chromatography	10
Mass spectrometry procedure	11
Data analysis	11
<hr/>	
Results and discussion	12
Method and instrumental performance	12
Experimental methanogen cultures	13
Ni isotopes at the Tekirova Ophiolite	16
Microbial life on the Tekirova ophiolite	19
<hr/>	
Conclusion	21
<hr/>	
Martian methane and astrobiology	22
<hr/>	
Acknowledgements	24
<hr/>	
References	25
<hr/>	
Appendix A - Reagents and solutions used in Ni elution	28
Appendix B - Cell culturing and preparation	29
Appendix C - Ni elution method	32

1. Introduction

Throughout Earth's history methane (CH_4) has played a key role in developing and regulating Earth's atmosphere and climate (e.g. Konhauser et al., 2009; Kasting, 2005). Especially during the Archaean, when the atmosphere was suggested to be still anoxic, a global CH_4 cycle flourished, exerting a great influence on the early Earth's atmosphere. The decimation of the global CH_4 cycle may be directly linked to the large scale oxygenation of Earth's atmosphere, known as the Great Oxidation Event (GOE), which took place approximately 2.45 Ga (e.g. Konhauser et al., 2009; Konhauser et al., 2015). In addition, CH_4 is not only found on Earth, but also in the atmospheres of many other bodies throughout our solar system, such as Mars (e.g. Hoefen et al., 2003; Mumma et al., 2009, Webster et al., 2015) and Titan (e.g. Kuiper, 1944, Hanel et al., 1981) sparking further interest to search for potential extraterrestrial life. After all, up to 80% of terrestrial CH_4 is thought to be emitted by living microbes (Etiope et al., 2011b).

Responsible for this high CH_4 atmosphere of the Early Earth is the process of methanogenesis, the production of CH_4 as a result of chemical reactions, either biotic or abiotic. Biotic methanogenesis, which we will be the main focus here, is a process carried out by methanogenic Archaea (methanogens). The oldest fossil evidence for methanogens based on molecular lipid biomarkers, dates back to 2.8 Ga (Brocks et al., 1999; Baptiste, 2005). This supports the significance of methanogens to the Archaean Earth and our need to comprehend biotic methanogenesis if we wish to unravel the climates and atmospheres of the Archaean Earth. Phylogenetic analysis of the methanogens indicates that they share the same main metabolic reactions (Baptiste, 2005), especially in the final steps where free CH_4 is produced (Ragsdale, 2009). Even though different methanogens use different substrates for this pathway, their key enzymes are roughly the same and have been well conserved throughout evolution. This implies that this metabolic process arose only once during evolution and that all modern methanogens share a common ancestor.

Methanogens require several specific Ni-bearing enzymes and cofactors for their metabolism. This Ni-dependence of methanogens suggests a potential link between available oceanic Ni and global CH_4 cycling. Such a link has been observed in Precambrian Iron Formations (IF). IFs show a strong drop in Ni-Fe ratios across the GOE (Konhauser et al, 2009, 2015). A strong depletion of oceanic Ni, known as the Archaean Ni famine, may have led to a strong decrease in methanogenic activity and CH_4 production, allowing for atmospheric O_2 to rise.

The role of Ni during methanogenesis and its fractionation patterns, implies it has a biomarker potential (Cameron et al., 2009). To determine if Ni isotopes can indeed be used as a biomarker, we analyzed environmental samples from location where methanogen presence can be confirmed. For this we focussed on the surface of the Tekirova ophiolite, Yanartas, Turkey..

Based on previous experimental work on Ni isotopic fractionation patterns during methanogenesis, we analyzed the Ni isotopic fractionation in controlled pure cultures of several methanogenic Archaea and in environmental samples from an active CH_4 seep. Isotopic analyses were performed at the Ifremer Centre de Bretagne, Brest, France. Our objectives were to (a) study biotic fractionation of Ni under different conditions, (b) determine Ni isotopic compositions of rocks and fluid seeps on the Tekirova ophiolite, Turkey, (c) assess the reliability of Ni isotopes as a biosignature, (d) speculate on a partially biogenic origin of CH_4 escaping the Tekirova ophiolite, and (e) discuss the validity of Ni isotope signatures as future a tool in astrobiology.

2. Background: Nickel and methanogenesis in nature

2.1. Ni isotopes

Ni is a common transition metal with atomic number 28 and has an average atomic mass of 58.7u. Valence states of Ni can be anywhere between 0 to 4+; however, only the 2+ state is encountered in natural systems. The absence of other valence states sets it apart from other metals like Fe: 2+ or 3+ and Cu: 1+ or 2+. Ni has five stable isotopes which we encounter in nature: ^{58}Ni , ^{60}Ni , ^{61}Ni , ^{62}Ni and ^{64}Ni , with abundances of respectively 58%, 26%, 1.1%, 3.6% and 0.9% (Gueguen et al., 2013). The most abundant isotopes ^{58}Ni and ^{60}Ni are frequently used in studying Ni isotopes. Though data on Ni isotopes is very limited, multiple water reservoirs, terrestrial reference materials, and rocks have been analysed (e.g. Gueguen et al., 2013; Cameron and Vance, 2014). In addition, fractionation patterns have been studied in ultramafic weathering (Ratié et al., 2015), biotic processes (e.g. Cameron et al., 2009) and abiotic processes (e.g. 2007; Fujii et al., 2011; Wasylenki et al., 2015).

2.2. Ni isotopes throughout the Earth

Ni isotopic compositions of multiple geological reference materials and hydrosphere reservoirs have been determined (Gueguen et al., 2013; Cameron and Vance 2014) using material NIST SRM 986 as a universal standard (see **Fig. U** and **Fig. T** for a visual compilation). $\delta^{60}\text{Ni}$ values of basalt, peridotite, and dunite reference materials range between -0.10‰ and +0.15‰. In contrast, low Ni granite is more ^{60}Ni enriched, exhibiting a much higher value of +0.43‰. Deep marine clays show near zero $\delta^{60}\text{Ni}$ values of +0.02‰ to +0.04‰. Organic rich sediment and coal display large ^{60}Ni enrichment with $\delta^{60}\text{Ni}$ values of respectively +0.58‰ and +0.47‰. Mn-nodule reference material from the Atlantic and Pacific have large positive $\delta^{60}\text{Ni}$ values of +1.03‰ and +0.36‰. The large spread between these values implies that Ni isotopic fractionation is sensitive to nodule forming processes. Additionally, a Banded Iron Formation (BIF) (3.8Ga) was found to be ^{60}Ni enriched with a $\delta^{60}\text{Ni}$ value of +0.45‰ (Gueguen et al., 2013). Little is known about Ni isotopic values of the hydrosphere (Cameron and Vance, 2014). Modern riverine $\delta^{60}\text{Ni}$ values are sparse and range between a minimum of +0.29‰ for the Amazon and Brahmaputra and a maximum of +1.34‰ for the Yangtze. Modern seawaters exhibit even higher $\delta^{60}\text{Ni}$ values and lie within a much smaller range of possible values. Analyses of seawater from the Atlantic, Pacific and Indian oceans shows compositions ranging from +1.21‰ to +1.58‰. Combining separate seawater isotopic compositions yield a general $\delta^{60}\text{Ni}$ value of $+1.44 \pm 0.15\%$ (2SD, n=27) (Cameron and Vance, 2014).

2.3. Abiotic Ni fractionation

Multiple processes are accountable for the fractionation of Ni and are observable in both experiments and in nature. A major control on Ni isotope fractionation is adsorption to particles. Particles in water columns or soils can exhibit a strong preference for light Ni. In soils and weathered rocks, Fe oxides and clays act as great scavengers of light Ni (Ratié et al., 2015). Due to the sorption of light Ni to these particles, Ni isotope compositions across weathering profiles show more negative $\delta^{60}\text{Ni}$ values with an increase in weathering grade. Recent experiments (Wasylenki et al. 2015) indicate that ferrihydrite acts as a strong scavenger of light Ni in the oceans, fractionating Ni through sorption processes. Another source of Ni fractionation, which is of great importance to understanding modern and ancient ocean chemistry, is Ni speciation in seawater. Ni can be incorporated not only as a free Ni^{2+} ion, but speciates with other compounds to form e.g. $\text{Ni}(\text{H}_2\text{O})_6^{2+}$, $\text{NiCl}(\text{H}_2\text{O})_5^+$, and $\text{NiCO}_3(\text{H}_2\text{O})_4$ (Fujii et al., 2011). In addition, Ni can sorb to organic ligands in seawater, again exhibiting a significant preference for lighter Ni. Fractionation between

free Ni, other Ni species, and Ni captured in marine sediments is key to reconstructing Ni isotopic compositions of seawater over time.

2.4. Biotic methanogenesis and Ni fractionation

The process of methanogenesis consists of multiple reaction steps, requiring enzymes, cofactors, and electron carriers. Some of these are relatively uncommon and found in all methanogens (Ferry, 2010). In methanogenesis a substrate, which can be a range of carbon bearing molecules, e.g. acetate or CO₂, is converted anaerobically to CH₄. This conversion is linked to the synthesis of ATP, providing the organisms' energy. A number of these used enzymes and cofactors requires a Ni atom (Watt & Ludden, 1999), which can be absorbed by methanogens through a special Ni processing system. During methanogenesis, Ni-bearing hydrogenase is used to oxidize H₂ (Ragsdale, 2009) and the freed electrons are used to reduce carbon-based molecules. Not only is Ni incorporated in Ni-bearing hydrogenase, but the metabolic step accounting for production of CH₄ can only occur through a reaction catalysed by the Ni-bearing enzyme Methyl-CoM Reductase (Thauer, 2010; Shima et al., 2012; Ragsdale, 2009).

When using a chemical element, organisms generally prefer one isotope to the other, resulting in fractionation between an organism and its environment. This phenomenon has been used extensively for elements such as C, N, S, and Fe. Only recently the non-traditional Ni isotope system has received interest. So far, studies into biotic Ni fractionation have focussed on methanogenic Archaea (e.g. Cameron et al., 2009; Fujii et al., 2011; this study), though fractionation of Ni isotopes has also been tested for other microorganisms. Growth experiments (Cameron et al., 2009.; Neubeck and Cameron, unpublished) suggested that methanogens exhibit a strong preference for the lighter ⁵⁸Ni, compared to the heavier ⁶⁰Ni, yielding large negative δ ⁶⁰Ni values exceeding -1‰ (Cameron et al., 2009; this study) or even -2‰ (Neubeck and Cameron, unpublished data).

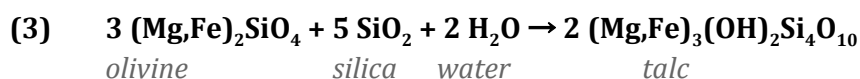
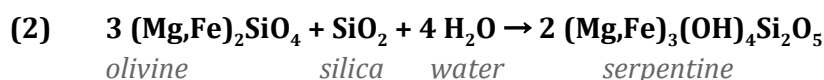
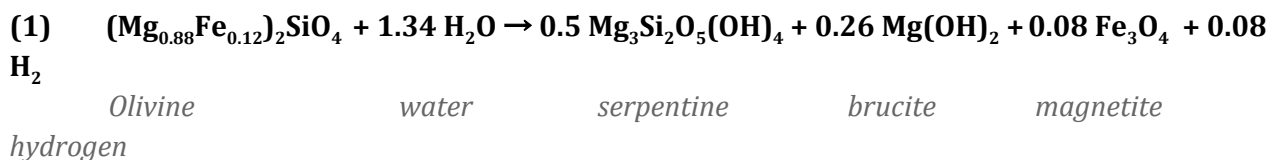
2.5. Oceanic Ni across the GOE

Having established that Ni is invaluable to all methanogens, we may use it to shed light on the Great Oxidation Event, or GOE. We already know that before the GOE Ni concentrations were much higher than after the GOE (Konhauser et al., 2009). This may have led to a decline in methanogen occurrence and productivity. Prevalence of methanogens and hence prevalent bioassimilation of Ni may leave a reservoir enriched in heavy Ni (Wasylenki et al., 2015). If the pre-GOE oceans Ni budget was strongly affected by Ni captured in biomass, pre-GOE oceans may have been more enriched in heavy Ni than post-GOE oceans. If this is the case, this would be reflected in BIFs across the GOE, i.e. δ ⁶⁰Ni values in BIFs would decrease over the GOE as ocean waters became less enriched with heavy Ni. Currently there is not enough Ni isotopic data of BIFs to test this hypothesis.

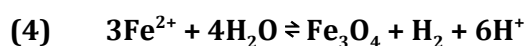
2.6. Methanogenesis on Earth through serpentinization

Methanogens are not the only producers of CH₄ on Earth. Abiotic processes can produce large amounts of CH₄ as well, as can be seen on the Tekirova ophiolite. The burning gas seeps of the Tekirova ophiolite are characterized by CH₄ (87%), H₂ (7.5-11%) and trace gases, including N₂, light alkanes, CO₂ and He (Hosgörmez, 2008.; Etiope et al., 2014). CH₄ seeps are often linked to leakage of thermogenic gas from pressurized subsurface hydrocarbon accumulations, but in ophiolites CH₄ seeps are believed to be the result of abiotic CH₄ production through serpentinization of the mafic host rock (Hosgörmez et al., 2008; Hosgörmez, 2007). In this case CH₄ is a product of reactions between olivine, H₂O, and carbon compounds, assisted by catalytic elements or minerals.

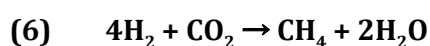
Serpentinization is a weathering process in which olivine, a solid solution between forsterite (Fo) and fayalite (Fa) is hydrolysed. In ultramafic rocks, olivine (here assumed to be Fo 0.88, Fa 0.12) and water react to form Mg-serpentine (1). Brucite and magnetite are byproducts and used as a sink for the surplus Fe and Mg from the olivine. In addition, small amounts of H₂ are produced (Neubeck et al., 2014). In more Si-rich rocks, such as basalt, olivine reacts with water and silica to serpentine (2) and talc (3) (Neubeck et al., 2014; Hietanen, 1973)



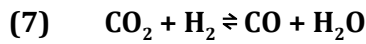
H₂ production can be explained through the oxidation of Fe²⁺ in the solid state and H₂O reduction (4). Simple thermodynamic calculations (Neubeck et al., 2011) of H₂ production through this process yield negative ΔG values at both high and low temperatures and with a pH range of 7 to 10 (ΔG = -100 to -200 kJ/mol at T=303K; ΔG = -150 to -275 kJ/mol at T=343K), indicating some extent of negligibility of temperature in this process, as the reaction is thermodynamically favourable at both high and low temperature. However, these calculations only predict thermodynamic favorability when Fe²⁺ is indeed in the solid state and the activity is thus 1. If the value for activity is lowered, e.g. when the species are present in a dilute solution, ΔG becomes positive (+46 kJ/mol) and the reaction becomes thermodynamically unfavorable.



As mentioned before, serpentinisation results in the production of H₂. Produced H₂ can under certain circumstances react with carbon in the rock, either as contained CO (e.g. Neubeck et al., 2011), CO₂ (e.g. Etiope et al., 2011a; Neubeck et al., 2011) or even carbonaceous solids, such as graphite (Hosgörmez, 2007). These reactions may yield abiogenic hydrocarbons such as CH₄, through multiple possible reaction pathways (e.g. Neubeck et al., 2011). The reaction of CO and H₂ (5^a and 5^b), known as the Fischer-Tropsch reaction (FTr) produces alkanes (C_nH_{2n+2}), including CH₄, depending on the stoichiometry of the reaction (a²). The reaction between CO₂ and H₂ (6) is known as the Sabatier reaction, a Fischer-Tropsch Type reaction (FTTr) and yields only CH₄. The FTr, FTTr, and Sabatier reaction require catalysts in the form of transition metals, e.g. Fe, Ni, Co, Ru, Cu, Zn. The composition of the hydrocarbons and the formation temperature depend on the catalysts present (Hosgörmez, 2007).



The rate and amount of hydrocarbon production are positively related with the presence of CO, rather than CO₂. Under the presence of a catalyst, CO₂ can react with H₂ to CO (7) (Seewald et al., 2005). This is known as the water-gas shift reaction (WGSR). Because of CO's higher potential to produce CH₄, it can be assumed that the WGSR is an important first reducing step in the FTr.



The production of CH₄ has been frequently proven at high temperatures (e.g. Etiope et al., 2011a, Neubeck et al., 2015), but a large range of temperatures allows for serpentinization and FTTrs. They can take place on Earth at temperatures well below 100°C, such as continental serpentinizing systems, or at temperatures over 200°C, like we can find near serpentinizing systems of mid-oceanic ridges (Neubeck et al., 2015). Recent low-temperature (30°C to 70°C) lab experiments of olivine weathering have indicated significant production of CH₄ at temperature regimes more applicable to the Earth's surface and where microbial activity can be present (Neubeck et al., 2011). CH₄ volumes produced in laboratory experiments are linearly related to the Si content of the growth medium. This implies that CH₄ is produced as a result of silicate weathering and H₂ production.

Seeping of CH₄ at the Tekirova ophiolite is characterized by the larger burning seeps in the hills. The macro-seeps eject typically 10⁵ to 10⁶ mg CH₄/m²/d. Cumulative emission of the macro-seeps is determined to be about 60,000 to 100,000 kg of CH₄ per year (Etiope et al., 2011a). In addition, widespread diffuse microseepage occurred throughout the area at invisibly small seeps. Here CH₄ seeps at much smaller rates: <<1 to 1 mg CH₄/m²/d (Etiope et al., 2011a).

2.7. Geology of the Tekirova ophiolite

The methane seeping outcrop of the Tekirova ophiolite lies along the southern edge of the ophiolite outcrop (Fig. 1). The area is characterized by the Late Cretaceous, ultramafic, Tekirova ophiolite, bound to Paleozoic-Mesozoic basement limestones. The Tekirova ophiolite belongs to the Neotethyan ophiolite, which surfaces around the Mediterranean.

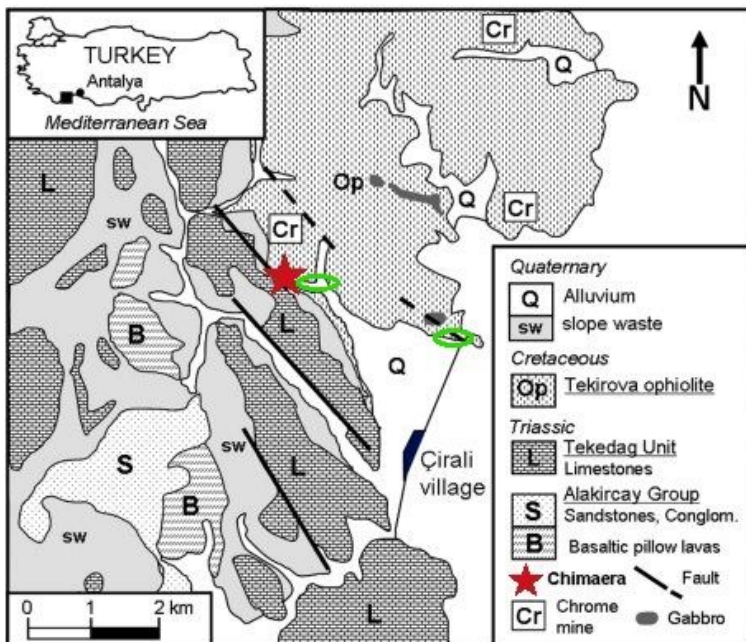


Figure 1. Geology of the Tekirova ophiolite, after Etiope 2011a. Area of large methane seeps is indicated by the red star. Green circles indicate zones with confirmed microseepage, measured and reported in Etiope, 2011a. Dispersed microseepage is however expected throughout the area.

3. Materials and Methods

3.1. Sample description

Several types of samples are studied: cell material from culture experiments, rock samples from an outcrop of the Tekirova ophiolite, water samples from fluid seeps on an outcrop of the Tekirova ophiolite, and solid and liquid samples from co-precipitation experiments of Fe oxides.

Cell material - Methanogens cultured in controlled environments were used here to create sufficient amounts of pure methanogen cell material. Cells were cultured at the Department of Microbiology, Swedish University of Agricultural Science, Uppsala.

Cultures consisted of 3 pure methanogen strains: the MAB1 strain of *Methanoculleus bourgensis* (MAB1), *Methanosarcina barkeri* (*M. barkeri*, DSM 800) and *Methanobacterium bryantii* (*M. bryantii*, DSM 10113). Cultures of *M. barkerii* and *M. bryantii* were provided by the Leibniz Institute DSMZ, the German Collection of Microorganisms and Cell Cultures. A MAB1 culture (Schnürer et al., 1994) was provided by the Department of Microbiology, Swedish University of Agricultural Sciences, Uppsala.

Cell material from 2 different experiments were analysed. The first experiment focused on the relation between Ni availability and CH₄ production. The second experiment investigated the excretion of metabolites by methanogens (see **Appendix B** for descriptions of the experiments). Growth media were carefully prepared as explained in **Appendix B**. To accurately determine Ni dependence and isotopic fractionation of the different methanogens, the only Ni source in the cultures was a carefully assembled trace metal solution. After growth media were prepared and injected into flasks, the flasks' atmospheres were replaced by an H₂-CO₂ mixture (20%-80% at 1 atm) and aliquots of the pure cell cultures were injected into the bottles. Cells were cultured in the dark at 37°C. After 119 days this atmosphere was refreshed and cells were harvested after 168 days.

Sorption and co-precipitation of Ni in ferrihydrite - To investigate the behaviour of Ni during coprecipitation with and sorption to ferrihydrite, precipitation experiments were performed. Experiments covered multiple Ni concentrations between 100 and 4000nM and Si concentrations of 0, 0.67 and 2.20mM. The produced ferrihydrite was separated from the solution through centrifugation. Precipitates were split. Part was analyzed for Ni isotopes, part was dried and analyzed using XRD for mineral composition. Experiments in progress, isotope data are expected in August 2016

Fluid seep samples - Samples were taken from fluid seeps. Sampling was performed during good weather to avoid mixing with rain water. Water was drawn slowly into sterile syringes and injected into acid cleaned plastic vials, filled with approximately 5 µl concentrated HNO₃. 11 fluid samples were collected.

Rock samples - Solid rock samples were taken by breaking of fresh rock and storing in sealed plastic bags. Sediment samples were scooped into clean falcon tubes. Solid rock samples from six sampling locations (**Fig. 2** and **Table 1**) were powdered for XRD and isotope analysis. Splits of the rock powders were dissolved.

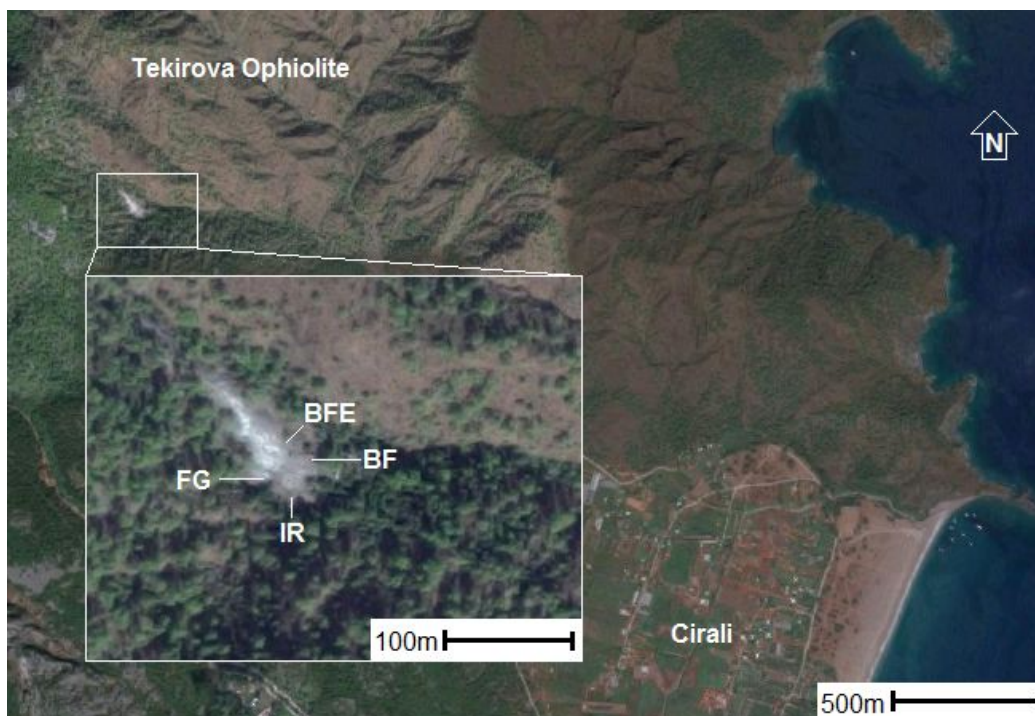


Figure 2. Sampling sites and location of the Tekirova ophiolite outcrop

Rock sample	Appearance
BF Travertine	Grey to rusty biofilm and travertine with small terracettes at the end of a small rill.
BFE-W	White material from ophiolite rocks penetrated by brucite veins.
BFE-B	Black material from ophiolite rocks penetrated by brucite veins.
FG6	White precipitates from a small rill with upwelling sources uphill and at the sampling site.
FG7	Rusty colored precipitates from a small rill with upwelling sources uphill and at the sampling site.
IR	Rusty colored precipitates from a small rill with an upwelling source uphill.

Table 1. Summary of rock samples.

3.2. X-ray diffraction

X-ray diffraction (XRD) was performed using a Powder diffractometer Panalytical X'Pert alpha1 at the Department of Material and Environmental Chemistry of Stockholm University. Powdered samples of all rock samples from the Tekirova ophiolite were analyzed for major mineralogical composition on all rock samples from the Tekirova ophiolite. Larger samples were analysed using conventional sample backloading and small volume samples were placed on a zero-background silicon wafer. We used the Search & Match function of the HighscorePlus software to identify minerals in the samples.

3.3. Mass bias, interference, and the ⁶¹Ni-⁶²Ni double spike

Multiple problems arise in determining the exact isotope ratios in natural samples. First of all during sample chemistry as the Ni elution process can fractionate Ni isotopes. Secondly, during mass spectrometry, Ni is fractionated as a result of instrument functioning (Albarede & Beard, 2004; Rudge et al., 2009), known as mass bias. Before ionisation in the Ar plasma, a liquid sample is vapourised to form a fine aerosol. As yield of the aerosol can be low, fractionation during this process should be taken into consideration. As the instrument works under a near vacuum and the sample is ionised under atmospheric pressure, a pressure gradient exists between different internal environments in the instrument. Between different pressure environments, lighter Ni isotopes diffuse more easily than heavier isotopes and are therefore preferentially lost. In addition, positive space charging occurs due to the concentration of positive ions in the beam. As a result of this positive charging, the positively charged Ni ions can be repelled from the sample beam, in which lighter positive Ni ions are repelled more easily than heavy Ni ions (Albarede & Beard, 2004). Lastly, isobaric interferences exist for all Ni isotopes (Gueguen et al., 2013): 58 (e.g. ⁵⁸Fe and ⁴⁰Ar¹⁸O⁺), 60 (e.g. ⁴⁴Ca¹⁶O⁺), 61 (e.g. ³⁶Ar²⁵Mg) and 62 (e.g. ³⁶Ar²⁶Mg), see **Table 2**. Just like the other problems, these interferences too can be corrected by double spiking, which will be explained below.

Interferences at mass (u)				
58	60	61	62	64*
⁴⁰ Ca ¹⁸ O	³⁶ Ar ²⁴ Mg ⁺	³⁶ Ar ²⁵ Mg ⁺	³⁶ Ar ²⁶ Mg ⁺	⁶⁴ Zn
⁵⁸ Fe	⁴⁴ Ca ¹⁶ O ⁺	³⁸ Ar ²³ Na ⁺	³⁸ Ar ²⁴ Mg ⁺	
²³ Na ³⁵ Cl ⁺			⁴⁶ Ca ¹⁶ O ⁺	
⁴² Ca ¹⁶ O ⁺				
⁴⁰ Ar ¹⁸ O ⁺				

Table 2. Interferences of elements, argides and oxides at mass 58, 60, 61, 62 and 64u.

*As ⁶⁴Ni was not measured, interference at mass 64u does not apply.

Isobaric interference from ⁵⁸Fe on ⁵⁸Ni is corrected by deriving ⁵⁸Fe from the constantly measured ⁵⁷Fe. The ⁵⁸Fe/⁵⁷Fe ratio in the sample is calculated from the natural ⁵⁸Fe/⁵⁷Fe ratio and taking into account the instrumental fractionation factor *fFe* of 1,35 between ⁵⁷Fe and ⁵⁸Fe (Eq. 1, after Gueguen et al., 2013). Rearrangement of Eq. 1 gives us a value for ⁵⁸Fe_{measured} (Eq. 2). This is subtracted from the total signal on mass 58, revealing the true signal of ⁵⁸Ni.

$$(1) \left(\frac{{}^{58}\text{Fe}}{{}^{57}\text{Fe}} \right)_{\text{measured}} = \left(\frac{{}^{58}\text{Fe}}{{}^{57}\text{Fe}} \right)_{\text{natural}} * \left(\frac{M_{58}}{M_{57}} \right)^{fFe}$$

$$(2) {}^{58}\text{Fe}_{\text{measured}} = \left[\left(\frac{{}^{58}\text{Fe}}{{}^{57}\text{Fe}} \right)_{\text{natural}} * \left(\frac{M_{58}}{M_{57}} \right)^{fFe} \right] * {}^{57}\text{Fe}_{\text{measured}}$$

To solve the problems that arise during mass fractionation, a double spike is used. The double spike method is commonly used in isotope geochemistry for many elements. It is proven a solid method for e.g. Ni (Gueguen et al., 2013), Ti (Millet et al., 2013), and Mo (Siebert et al., 2001) isotopes. A

predetermined amount of double spike is added to all samples, standards and blanks before Ni elution. The double spike method involves 4 isotopes, of which 2 are artificially enriched: ‘spiked’. From the relative abundances of the isotopes and by knowing the double spike composition, mass bias corrected true isotope ratios can be derived (Rudge et al., 2009). For the Ni isotope system, a ^{61}Ni - ^{62}Ni spike is optimal. ^{61}Ni and ^{62}Ni are rare, with abundances of respectively 1.1 and 3.6% (Gueguen et al., 2013; Gall et al., 2012). There are no common isotopes of mass 61 and 62 to isobarically interfere with ^{61}Ni and ^{62}Ni during mass spectrometry. A ^{61}Ni - ^{62}Ni double spike (51.29%-46.61%) was used. To maximize the effect of the double spike, the total amount of Ni introduced through the double spike is aimed to be equal to the total amount of Ni in the sample; one of the reasons Ni concentrations are determined before Ni elution. The double spike method, however, allows for some deviation in this mixing ratio and optimal results are obtained as long as the $\text{Ni}_{\text{natural}}/\text{Ni}_{\text{spike}}$ ratio is within 0.5 and 2.

The composition of the double spike was determined by comparison to an isotopic standard: NIST SRM 986, which in turn was analyzed using pure single isotope calibration. The composition of the NIST SRM 986 standard (Gramlich et al., 1986) and the double spike (Gueguen et al., 2013) can be found in **Table 3**. Errors are in 2SD.

Isotope	Abundance	
	NIST SRM 986 (%)	Double spike (%)
^{58}Ni	68.07689 ± 0.00592	1.05106 ± 0.00071
^{60}Ni	26.22315 ± 0.00514	0.76947 ± 0.00071
^{61}Ni	1.13989 ± 0.00043	51.28893 ± 0.04432
^{62}Ni	3.63453 ± 0.00114	46.61106 ± 0.04753
^{64}Ni	0.92555 ± 0.00060	0.27920 ± 0.00055

Table 3. Abundances of isotopes in the NIST SRM 986 standard (Gramlich et al., 1989) and the used ^{61}Ni - ^{62}Ni double spike (Gueguen et al., 2013)

There are multiple advantages to using the double spike method. It increases the concentration of the rare Ni isotopes at mass 61 and 62, enhancing the detection capabilities of the detectors and the software’s statistics. It also enables us to determine the yield of the chromatography procedure and the fractionation during Ni elution and instrumental mass bias.

Blank samples were spiked and underwent the same Ni elution procedure as other samples, illustrating potential fractionating processes during chemistry and spectrometry. Blanks also indicated that no significant signal existed at mass 58 without a sample present, implying that no ^{58}Ni was present in chemical reagents used in the elution process and no Ni was contributed by the Ni sample and skimmer cones.

3.4. Ni elution through liquid column chromatography

Sample preparation was performed in a clean room (Class 1000, or ISO-6) at the Ifremer Bretagne Centre, Brest, France. Ni was eluted using liquid column chromatography. The procedure was performed on both seeped fluids and a number of rocks/precipitates. The Ni elution method is a

slight modification from Gueguen et al., 2013, which was performed at the same laboratory. A detailed step by step explanation of the method can be found in **Appendix C**.

During HF dissolution, precipitates formed in the vials, assumably fluoride salts, such as CaF. A well mixed split of precipitate and solution was taken prior to Ni elution, as well as a split of clear solution after centrifuging the samples. This was performed in order to find the most representative $\delta^{60}\text{Ni}$ value and determine if significant Ni fractionation occurred due to fluoride precipitation

To elute Ni, liquid samples were evaporated and residues dissolved by addition of 0.24M HCl, 0.2M ammonium citrate and concentrated ammonia. Chromatography columns were loaded with a Ni specific resin, which consists of microbeads covered in dimethylglyoxime(DMG). Ni binds to DMG to form the insoluble Ni-DMG complex, therefore trapping Ni on the microbeads. Matrix elements, such as Cu and Fe were washed off and discarded. The eluted Ni is then removed from the beads by rinsing with HNO_3 and collected in teflon vials. Eluted Ni solutions are evaporated to dryness, dissolved in 0.28M HNO_3 and transferred to vials for MC-ICP-MS.

3.5. Mass spectrometry procedure

Ni isotopic compositions were determined using a Thermo Scientific™ Neptune multicollector inductively coupled plasma mass spectrometer (MC-ICP-MS) at the Ifremer Centre de Bretagne in Brest, France. The instrument contains 9 Faraday cups, set to medium mass-resolution. The instrument simultaneously measures signals of ^{57}Fe , ^{58}Ni , ^{60}Ni , ^{61}Ni , ^{62}Ni , ^{63}Cu and ^{65}Cu . Samples are introduced using an ApexQ MicroFlow PFA-50 self-aspirating nebulizer at an injection rate of $\sim 60\mu\text{lmin}^{-1}$. The instruments sample and skimmer cones are made of Ni, but ^{58}Ni yield on the blanks indicate no Ni is contributed from the cones, as demonstrated before (Gueguen et al., 2013; Moynier et al., 2007)

Each set of 24 samples was run twice. A short preliminary run was performed to better determine Ni, Fe and Cu concentration. This run consisted of 10 injections per sample, each lasting 4 seconds. After this run, samples are ordered by increasing Ni concentration and additional standards were prepared. For every sample there was a standard with similar concentration and $\text{Ni}_{\text{spike}}/\text{Ni}_{\text{natural}}$ ratio. Samples were generally grouped in sets of 2 to 5 samples, preceded and succeeded by one bracketing standard of NIST-SRM-986 prepared to represent the sample group. The second, more thorough run was performed to find precise isotope data. Each sample was measured through 50 cycles of 4 seconds integration time each. Measurement were separated by an instrument rinse of 10 cycles of 4 seconds integration time. The number of values was reduced in 2 steps: first from 50 to 5, then from 5 to 1 definitive value.

The instrument can very precisely measure samples over 30ng Ni g^{-1} : $2\text{SE}<0.1$. Lower concentration measurements yield slightly larger uncertainties in δ -values, with $2\text{SE}\approx 0.1\%$. Only concentrations under 10ng g^{-1} have extremely high uncertainties exceeding 1% (Gueguen et al., 2013). Ni concentrations in rock samples were very high (>10 's of $\mu\text{g g}^{-1}$). Ni concentrations in water samples were generally sufficient ($20\text{-}100\text{ ng g}^{-1}$) though some were well below 30ng g^{-1} . Only one sample below 10ng g^{-1} , was analyzed isotopically.

3.6. Data analysis

To quantify fractionation of Ni isotopes, we determined ratios between the heavy isotope ^nNi , where $n=60, 61$ or 62 , and ^{58}Ni (Eq. 1), the lightest and most common isotope of Ni. We then used the

δ -notation (Eq. 2) commonly used in isotope geochemistry, with NIST SRM 986 as the standard for all samples. In particular $\delta^{60}\text{Ni}$ was used to compare natural samples to known reservoirs. When quantifying fractionation between methanogens and their growth media, $\delta^{60}\text{Ni}$ based on the NIST SRM 986 standard has no meaning. To be able to quantify fractionation between the two we used the $\Delta^{60}\text{Ni}$ value (Eq. 3).

$$(1) \quad R = \frac{{}^n\text{Ni}}{{}^{58}\text{Ni}}$$

$$(2) \quad \delta^n\text{Ni} [\text{‰}] = \left(\frac{R_{\text{sample}} - R_{\text{standard}}}{R_{\text{standard}}} \right) \times 1000 = \left(\frac{R_{\text{sample}}}{R_{\text{standard}}} - 1 \right) \times 1000$$

$$(3) \quad \Delta^{60}\text{Ni} = \delta^{60}\text{Ni}_{\text{cell}} - \delta^{60}\text{Ni}_{\text{medium}}$$

Although theoretically all $\delta^n\text{Ni}$ values can be determined, we focussed on $\delta^{60}\text{Ni}$. Due to the double spiking method, where ${}^{61}\text{Ni}$ and ${}^{62}\text{Ni}$ are used to correct for instrumental fractionation, which is mass dependent, all determined values for $\delta^{61}\text{Ni}$ and $\delta^{62}\text{Ni}$ will per definition fall on a mass dependent fractionation line, concealing any mass dependence of fractionated samples.

To determine the errors of the $\Delta^{60}\text{Ni}$ value calculated in **Eq. 3**, we used the ‘root of sum of squares’, or RSS method to propagate the errors (provided in 2SD) of $\delta^{60}\text{Ni}$ of the cell and the growth medium. The method calculates the root of the sum of all errors squared; it puts focus on the larger errors. This is portrayed in Eq. 4, with n errors of 2SD.

$$(4) \quad 2SD_{\text{new}} = \sqrt{\sum_{n=1}^n (2SD)^2_n}$$

4. Results and discussion

4.1. Method and instrumental performance

Considering all determined data points, including data obtained that are irrelevant to this study, we observe a negative relation between the amount of Ni in the vials and the error in the measurement. **Fig. 3** indicates this relationship, as the error (in 2SD) only exceeds 0.1‰ for samples containing less than 100ng total Ni. Below 100ng, the error decreases rapidly with an increasing Ni content. Above 100ng, on the other hand, the error stabilizes and no negative trend exists any longer between the Ni contents and the error. This pattern agrees very well with earlier Ni isotope measurements, using the same instrument and chemical procedure (Gueguen et al., 2013).

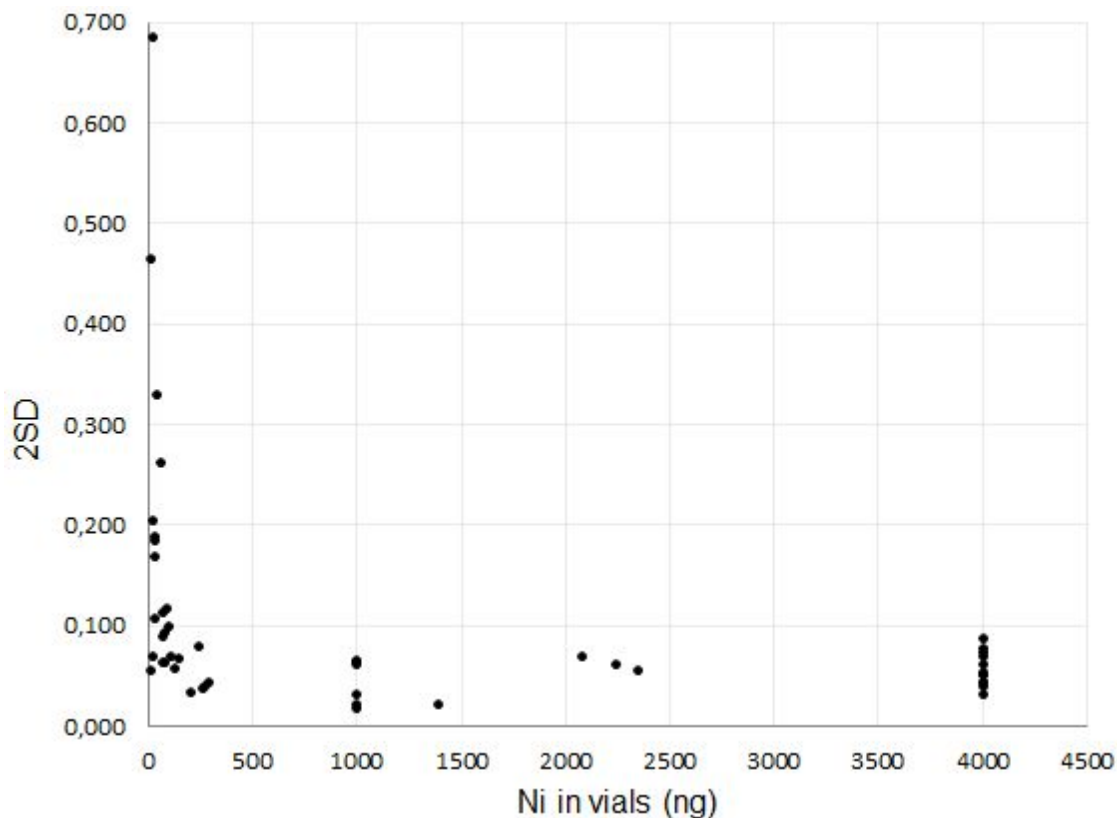


Figure 3. Plot of the error (2SD) vs. total Ni in the vials (ng). Clear is the steep decrease in error with rising Ni content up to ~100ng. Consequently low (<0.1%) errors apply to all samples containing over 100ng.

We analyzed both clear rock solutions and fluoride precipitates from the vials, to demonstrate if significant Ni fractionation occurs when fluoride precipitates form in the rock solution. This was not the case, as can be seen by the resemblance between the 2 values, illustrated in **Fig. W**. Suspensions and clear solutions agree well within error.

4.2. Experimental methanogen cultures

Collecting Ni isotope data from methanogen cultures was hindered by the low amounts of Ni in the cell pellets. Cell pellet solutions of the methanogenesis experiments generally contained low amounts of Ni (<50 ng per cell pellet) and therefore have relatively large errors. Quadrupole measurement indicated Ni amounts as low as 3.3ng per sample. $\delta^{60}\text{Ni}$ of samples containing 8ng Ni or less were not measured. Contrary to expectation, cell pellets did not unanimously show enrichment of light Ni as demonstrated by Cameron et al., 2009. When $\Delta^{60}\text{Ni}$ was determined using $\delta^{60}\text{Ni}$ of the cell pellets and their corresponding growth media, a number of experiments displayed a positive $\Delta^{60}\text{Ni}$ value (**Table 4** and **Fig. 4**). *MAB1* cultures indicated a positive $\Delta^{60}\text{Ni}$ value of ~0.5‰ for the standard growth medium and a strong negative $\Delta^{60}\text{Ni}$ value of ~-2.2‰ for the growth media with extra Ni addition. Cell pellets of *M. barkeri* were generally too low in Ni to determine the isotopic composition, but the experiment using the normal growth medium yielded cell with a very slight positive $\Delta^{60}\text{Ni}$ value of ~0,1‰. *M. bryantii* shows a strong positive $\Delta^{60}\text{Ni}$ of of ~1‰ for the low Ni growth medium, a lower, yet still positive $\Delta^{60}\text{Ni}$ ~0.5‰ for the normal growth medium and a slight negative $\Delta^{60}\text{Ni}$ value of ~-0.01‰. *MAB1* and *M. bryantii* experiments showed a decrease in $\Delta^{60}\text{Ni}$ values as the Ni concentration in the media increases, i.e. the more Ni in the media, the lighter the isotopic values in the cells.

Cell culture	Ni in sample (ng)	$\delta^{60}\text{Ni}$ cell (‰)	$\delta^{60}\text{Ni}$ medium (‰)	$\Delta^{60}\text{Ni}$ (‰)	2SD (‰)
MAB -Ni	8,0ng*	-	-0,026	-	-
MAB normal	10,8ng	-0,152	-0,658	0,506	0,088
MAB 1nM	27,6ng	-2,785	-0,559	-2,227	0,199
M. barkeri -Ni	3,3ng*	-	-1,16	-	-
M. barkeri normal	36,4ng	-0,626	-0,770	0,145	0,332
M. barkeri 1nM	6,2ng*	-	-0,67	-	-
M. bryantii -Ni	8,2ng	-0,094	-1,060	0,966	0,480
M. bryantii normal	27,9ng	-0,290	-0,805	0,515	0,113
M. bryantii 1nM	16,4ng	-0,667	-0,653	-0,014	0,690

Table 4. Collection of $\delta^{60}\text{Ni}_{\text{cell}}$, $\delta^{60}\text{Ni}_{\text{medium}}$, and $\Delta^{60}\text{Ni}$. Expected $\Delta^{60}\text{Ni}$ values are negative and marked in green. Unexpectedly high $\Delta^{60}\text{Ni}$ values, i.e. all positive values are highlighted red. Samples marked * are too low in Ni to be accurately measured.

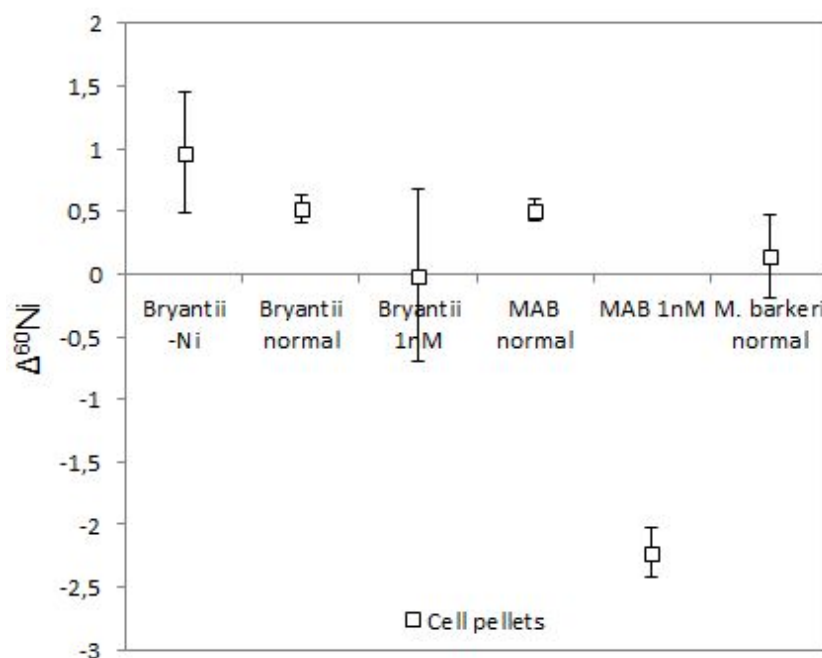


Figure 4. $\Delta^{60}\text{Ni}$ values of cell pellets from the CH_4 production experiments.

The latter observation hints at a possible concentration dependence of Ni isotope fractionation. Isotopic fractionation has been found previously to be dependent on nutrient availability. This was shown for example in nitrogen (N) isotopes during NH_4^+ uptake by phytoplankton (Kon-Kee et al., 2013), and in carbon (C) isotopes during CO_2 uptake by photosynthetic plankton (Freeman & Hayes, 1992). Fractionation generally increases as the nutrient in question is more highly abundant, i.e.

δ -values become more negative with increasing concentration. In a way, micro organisms become more 'picky' as there are more nutrients available. Though we cannot conclude this for Ni based on the few data points we obtained, the data does not contradict this and the extent of concentration dependent fractionation should be investigated.

Another way of explaining the positive $\delta^{60}\text{Ni}$ values can be that the data we obtained may have been negatively affected by problems arising from the cell harvesting method or from contamination during the harvesting or purification process. If Ni is lost during cell purification this may prefer loss of the lighter isotopes, leaving the cell pellets enriched in the heavier isotopes. This would explain the positive values, but it would not explain the apparent trend between the Ni concentrations and the $\delta^{60}\text{Ni}$ values. Also, this would require cell lysis, which is not expected to take place during cell pellet centrifugation

Additionally, the offset could be explained by the addition of organic ligands to the solution. Organic ligands are proven to be strong Ni scavengers (Fujii et al., 2011) and are capable of fractionating Ni to similar values as biological fractionation. To prevent this, no yeast extract was added to the growth media. However, the addition of clean cell culture inoculates may have strongly increased the concentration of organic ligands in the growth media which, unlike the cells, may have started scavenging lighter Ni right away, leaving the medium - and therefore the cells - enriched in heavy Ni. Later, during separation of cells and growth media, the lighter Ni may stay behind in the growth media adsorbed to the organic ligands. This process may also be responsible for the seeming concentration dependence of Ni fractionation. As there is a higher concentration of Ni in the growth media, the growth media will be less enriched in heavy Ni upon addition of organic ligands. In this case the decrease of $\delta^{60}\text{Ni}$ values with increasing concentration can be assigned to the decrease in enrichment of the growth media in heavy Ni, rather than differences in fractionation by methanogens.

Cell pellets from the metabolite experiment (**Table 5**) contain significantly more Ni (>200 ng per sample) than cell pellets from the methanogenesis experiment. Contrary to the cell culture experiment, summarized in **Table 4**, all cell pellets exhibit negative $\Delta^{60}\text{Ni}$ values. *MAB1* -Ni (in red) was excluded, as Ni content was impossibly high and contamination with another Ni source assumed. One additional data point is considered, which is *MAB1* normal (Cameron), a result from a previously unreported experiment, using the same methodology as our experiments.

Cell culture	Ni in sample (ng)	$\delta^{60}\text{Ni}$ cell (‰)	$\delta^{60}\text{Ni}$ medium (‰)	$\Delta^{60}\text{Ni}$ (‰)	2SD (‰)
MAB1 -Ni	1388,1ng	-0,735	-0,026	-0,709	0,136
MAB1 normal	292,4ng	-1,350	-0,777	-0,777	0,016
MAB1 normal	261,4ng	-1,393	-0,413	-0,980	0,054
MAB1 normal	237,5ng	-1,262	-0,413	-0,849	0,088
MAB1 normal (Cameron)		-2,32	-0,0116	-2,080	0,012

Table 5. Collection of cellular $\delta^{60}\text{Ni}$, $\delta^{60}\text{Ni}$ in the growth media and $\Delta^{60}\text{Ni}$. Samples exhibiting the expected negative $\Delta^{60}\text{Ni}$ values are highlighted in green. *MAB1* -Ni was excluded, as Ni content was impossibly high (in red) and contamination with another Ni source suspected.

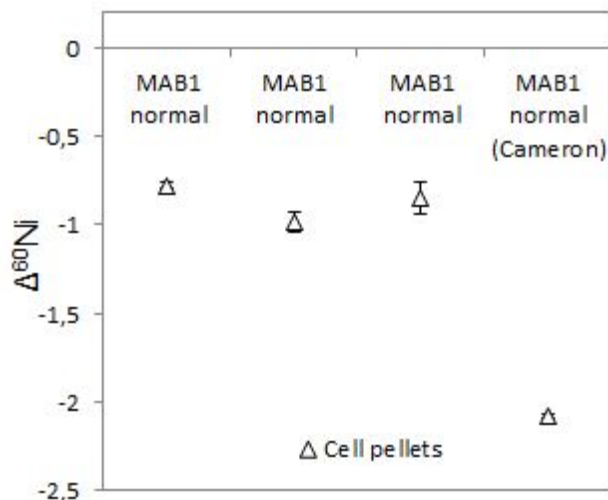


Figure 5. $\Delta^{60}\text{Ni}$ values of cell pellets from the metabolite experiment. In this case, all $\Delta^{60}\text{Ni}$ values are negative. The experiment by Cameron (Cameron, unpublished) shows a much larger negative $\Delta^{60}\text{Ni}$ value.

A potentially significant feature is the concentration dependence of Ni fractionation. Due to the low number of data, it is not possible to conclude that Ni isotope fractionation is dependent on the Ni concentration in the media, but the data suggest that negative Ni isotopic excursions only occur when Ni concentrations are sufficient (**Fig. 4**), and larger negative excursions occur when the Ni concentration is increased (**Fig. 5**). Missing from our experiments are data on the change of isotopic composition over time. In earlier similar experiments the growth media were sampled over time and an increase in $\delta^{60}\text{Ni}$ was found for the growth media as the cell cultures developed (Cameron et al., 2009), implying an increasingly negative $\delta^{60}\text{Ni}$ as cultures grow.

Now we need to question why the methanogen cell material does not exhibit the well known negative $\delta^{60}\text{Ni}$ signature. We can say with relatively certain that the Ni intake by methanogens prefers the light Ni and that the subsequent negative $\delta^{60}\text{Ni}$ signature is robust (e.g. Cameron et al., 2009; Fujii et al., 2011). When the process is reversed, i.e. cells lose Ni, we expect the lighter Ni to be preferentially lost and hence the $\delta^{60}\text{Ni}$ to increase. To explain the observed positive $\delta^{60}\text{Ni}$ values we need to consider the cell harvest method. Cells may have lost Ni due to the centrifuging and washing procedure. If loss of light Ni is preferred during the used methods, this can conceal the initial isotopic signature. Care must be taken in harvesting cell material to avoid deviating from initial isotopic composition.

Another problem that is encountered is the impossibility to discriminate between actual metabolic fractionation and simple fractionation due to the adsorption of Ni to the cells. Some Ni will have been fractionated by active transport into the cell via a Ni transport system, which is a metabolic, and hence biotic process. However, since Ni has the ability to adsorb to simple inorganic ligands (Fujii et al., 2011), we have to consider that Ni may fractionate by a similar process: abiotic adsorption onto organic molecules on cell surfaces. As there is no possibility to separate intracellular Ni from extracellular Ni we can not separate between metabolic Ni fractionation and surface speciation.

4.3. Ni isotopes at the Tekirova Ophiolite

Water and rock samples from the surface outcrops show a clear distinction in $\delta^{60}\text{Ni}$ values. Fluid samples were much more ^{60}Ni enriched and more variable in isotopic composition. $\delta^{60}\text{Ni}$ values ranged from +0.90‰ to +1.77‰ in fluids. The average fluid isotopic composition was $+1.26\text{‰} \pm 0.58\text{‰}$ ($n=9$, 2σ) and fluid samples were more ^{60}Ni enriched than rock samples. All $\delta^{60}\text{Ni}$ values of fluid samples were higher than any of the rock $\delta^{60}\text{Ni}$ values and the $\delta^{60}\text{Ni}$ values of fluids were less consistent. $\delta^{60}\text{Ni}$ values of rock samples plotted closer to 0‰, showing slightly positive values for 5 out of 6 samples. Their average $\delta^{60}\text{Ni}$ value is $+0.19\text{‰} \pm 0.26\text{‰}$ ($n=6$, 2σ). The rock sample $\delta^{60}\text{Ni}$ values showed a striking feature: site IR plots significantly lower in **Fig. 8** and exhibits a distinctly lower $\delta^{60}\text{Ni}$ value.

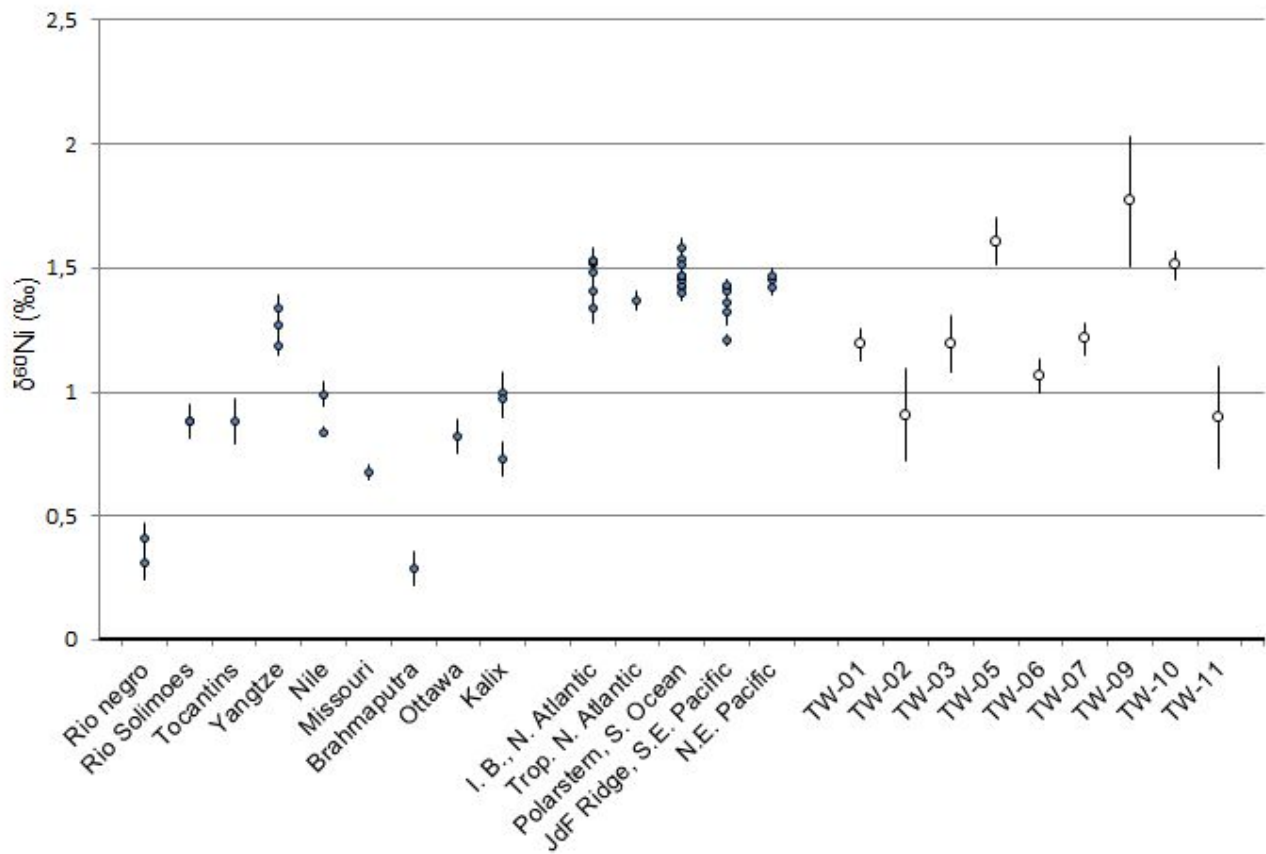


Figure 6. Collections of riverine and oceanic Ni isotopic compositions (After Cameron and Vance, 2014; blue markers) and Ni isotopic compositions from fluid seeps on the Tekirova ophiolite (open markers).

When comparing fluid seep values to known hydrospheric values, previously determined by Cameron and Vance, 2014, large differences are apparent. Riverine values throughout the world vary strongly, but within one river system $\delta^{60}\text{Ni}$ values are constricted to quite small ranges of well within 0.5‰ (see **Fig. 6**). Our values vary strongly on a much smaller scale, and within a few 100 meters across the outcrop nearly 1‰ deviation exists within $\delta^{60}\text{Ni}$. Our samples are generally more enriched in heavy Ni than riverine samples.

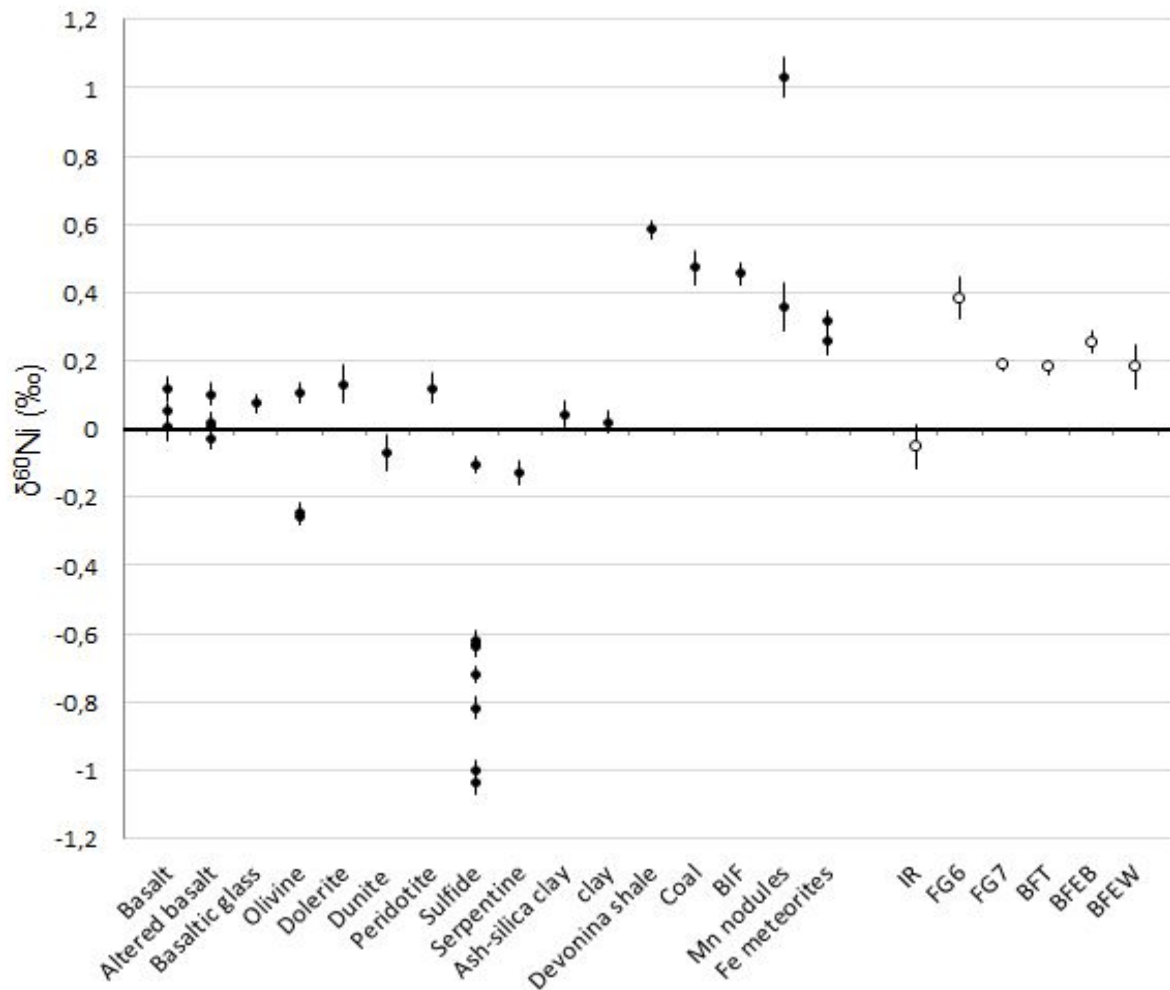


Figure 7. Collection of global Ni isotopic compositions of rock materials (After Gueguen et al., 2013; solid markers) and our own samples (open markers).

Our Ni isotopic data for rocks agree relatively well with known terrestrial values (see **Fig. 7**). 5 out of 6 samples are more ^{60}Ni enriched than mafic minerals and rocks and in general, our samples are less enriched in ^{60}Ni than sediments. However, when focussing more closely on alteration products in the table our rocks seem more ^{60}Ni enriched. Altered basalt and serpentine reference materials (date from Gueguen et al., 2013) plot close to 0‰, whereas most of our values, i.e. 5 out of 6, plot slightly higher than those references.

Care should be taken in trying to reveal a Ni biosignature in natural samples. A negative $\delta^{60}\text{Ni}$ value should not be confused with the negative $\Delta^{60}\text{Ni}$ value we find in experiments and hence a negative $\delta^{60}\text{Ni}$ value does not imply a biosignature on it's own and should always be compared to other values.

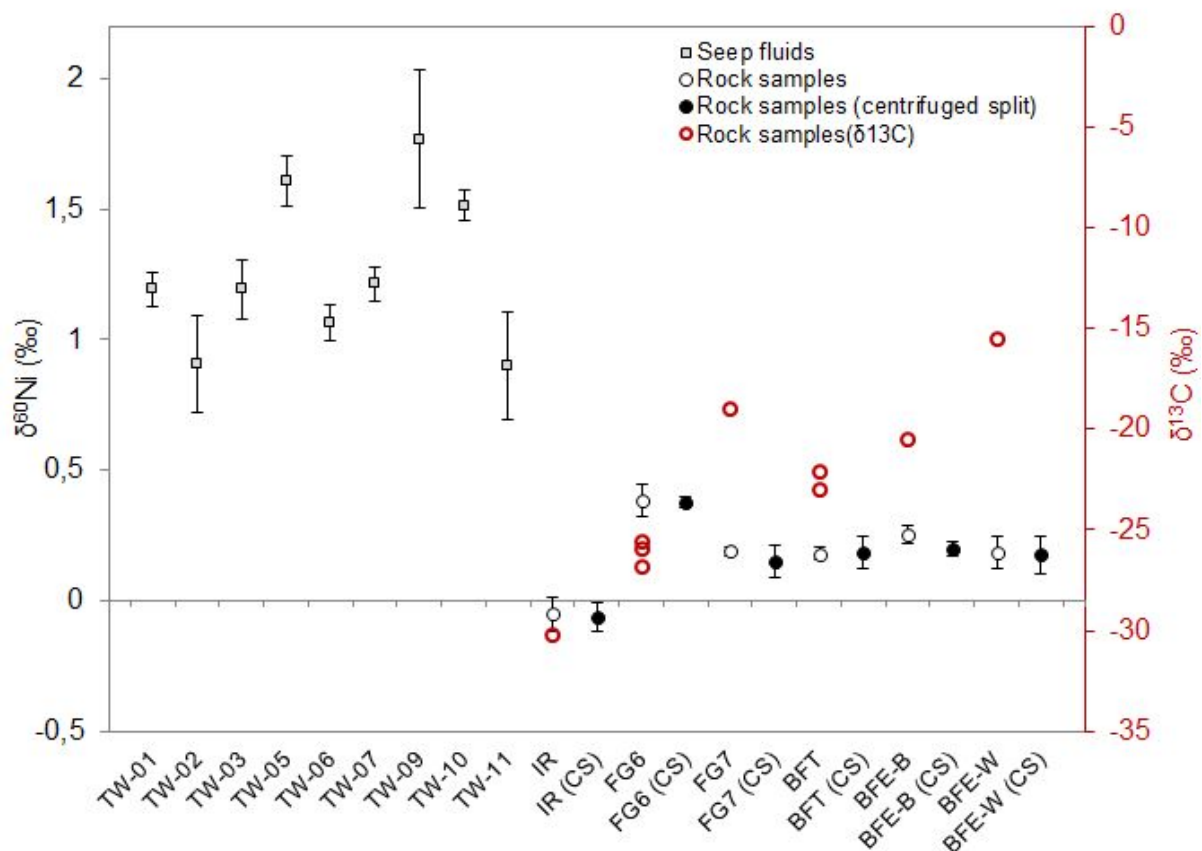


Figure 8. Compilation of $\delta^{60}\text{Ni}$ values of seep fluid samples (TW-01 to TW-11), fluoride suspension rock solutions (IR, FG6, FG7, BFT, BFE-B, BFE-W) and centrifuged clear rock solution samples (indicated by "(CS)"). Additionally, $\delta^{13}\text{C}$ values for rock samples are displayed

4.4. Microbial life on the Tekirova ophiolite

Earlier study (Meyer-Dombard et al., 2015) of the ophiolite outcrop indicated the outcrop surface and subsurface form an ecosystem, with a clear divide between microbial activity at the surface and in the subsurface. Aerobic heterotrophic micro organisms are found to dominate the surface and no anaerobic microbes, to which the methanogens belong, are found. However, samples were not immediately frozen, but frozen 2 hours after collection. Microbes were later cultured before DNA analysis was performed. This may have disturbed the microbe and possible negatively affect retrieval of DNA data.

Phylum	Order(o)/family (f)/genus (g)
Crenarchaeota	<i>Nitrososphaeraceae</i> (f) <i>Candidatus Nitrososphaera</i> (g) *
Euryarchaeota	<i>Methanobacteriaceae</i> (f) <i>Methanobacterium</i> (g)
Euryarchaeota	<i>Methanobacteriaceae</i> (f) <i>Methanobrevibacter</i> (g) ^{2,3}
Euryarchaeota	<i>Methanobacteriaceae</i> (f) <i>Methanosphaera</i> (g) ^{2,3}
Euryarchaeota	<i>Methanocellaceae</i> (f) <i>Methanocella</i> (g)
Euryarchaeota	<i>Methanosataceae</i> (f) <i>Methanoseta</i> (g)

Euryarchaeota	<i>Methanosarcinaceae</i> (f) ANME-3 (g)
Euryarchaeota	<i>Methanosarcinaceae</i> (f) <i>Methanosarcina</i> (g)
Euryarchaeota	E2 (o) ¹
Euryarchaeota	<i>Methanomassiliicoccaceaea</i> (f) <i>Methanomassiliicoccus</i> (g) ¹
Euryarchaeota	<i>Methanomassiliicoccaceaea</i> (f) <i>vadinCA11</i> (g) ¹
Parvarchaeota	WCHD3-30 (o) *
Parvarchaeota	YLA114 (o) *

Table 6. Summary of Archaea found on the surface of the Tekirova ophiolite. Non-methanogenic species and methanogens found on humans are marked red. Methanogens not known to be present on humans are marked green.

¹ Borrel et al., 2013

² Carbonero and Gaskins, 2013

³ Triantafyllou et al., 2014

⁴ Scanlan et al., 2008

* Not a methanogen

In contrast to these findings, a larger array of surface dwelling microbes has recently been presented (Neubeck et al., in prep.). This new array of microbes can be considered more reliable, as the sampling method included immediate freezing on dry ice in order to better preserve DNA. Additionally, DNA analysis was performed before culturing experiments. DNA analysis indicates presence of several groups of Archaea: *Parvarchaeota*, *Crenarchaeota* and *Euryarchaeota*, of which the latter harbours the methanogens. When using general primers, archaea made up <1% of the total microbial population in all but one sampled location (**Table 7**). Archaea that are found on humans (**Table 6**) are excluded from the found consortium to make sure no Archaea are reported that are a result from human contamination. Occurrence of methanogens, which are anaerobic microbes, at the surface is unexpected, as they are outcompeted by aerobic microorganisms. We therefore expect a more significant community of methanogens exists within the ophiolite, where we would expect to find anaerobic conditions. In addition, methanogens may thrive in biofilms or other small microenvironment, sheltered from oxygen.

Rock sample	Major mineral assemblage (score 1-100)	Euryarchaeota in % of total microbial population	$\delta^{13}\text{C}^*$	$\delta^{60}\text{Ni}$
BFT	Calcite (93)	0.01%	-22.15±0.15‰ -22.98±0.15‰ [†]	0.18±0.02‰
BFE - white	Brucite (91)	no presence	-15.56±0.15‰	0.18±0.06‰
BFE - black	Chrysotile (52) Mg ferrite (30)	no presence	-20.53±0.15‰	0.25±0.03‰
FG6	Aragonite (83) Calcite (35)	0.05%	-25.94±0.15‰ -25.61±0.15‰ -26.86±0.15‰ [‡]	0.38±0.06‰

FG7	Aragonite (82) Magnesian Calcite (45)	0.07%	-18.98±0.15‰	0.19±0.02‰
IR	Chrysotile (80)	0.03%	-30.19±0.15‰	-0.05±0.07‰

Table 7. Summary of rock sample mineralogy (mineral and XRD match score), methanogen presence, $\delta^{13}\text{C}$, and $\delta^{60}\text{Ni}$.

* $\delta^{13}\text{C}$ data of the solid samples after Neubeck et al., unpublished (in progress)

† $\delta^{13}\text{C}$ of respectively lower and upper part of site BFT.

‡ $\delta^{13}\text{C}$ of respectively white suspended sediments, white solid phase minerals, and darker sediments at site FG6

A biogenic origin of the Tekirova gas is not implied by the isotopic composition of the CH_4 itself. When comparing the $\delta^{13}\text{C}_{\text{CH}_4}$ and $\delta\text{D}_{\text{CH}_4}$ of the gas seeps from Tekirova with CH_4 seeps from well understood sources it becomes clear that the majority of the CH_4 must be abiotically formed (Etiope et al., 2011a). Microbial gas typically exhibits very strong ^{13}C and D fractionation. $\delta\text{D}_{\text{CH}_4}$ is typically well below -150‰ and $\delta^{13}\text{C}_{\text{CH}_4}$ lower than -40‰ in microbial gas. The CH_4 from Tekirova shows much weaker fractionation pattern with $\delta\text{D}_{\text{CH}_4}$ ranging from -100‰ to -150‰ and $\delta^{13}\text{C}_{\text{CH}_4}$ around -10‰. This does however not disprove the hypothesis of a partially biogenic origin, but it does imply that if there is a biogenic contribution, this is likely very minor.

Although at most sites Euryarchaeota were observed, not all do indeed harbour methanogens. At sites IR and FG7 methanogen occurrence was observed through anaerobic cultivation in lab, DNA analysis, and lipid analyses (i.e. archaeol and squalane). At all sites negative $\delta^{13}\text{C}$ values were found (ranging from -15.56‰ to -30.19‰). Due to the strikingly low $\delta^{13}\text{C}$ value at site IR (-30.19‰), a higher microbial activity was assumed here (Neubeck et al., in prep.). Correlating to this high methanogen activity was a much lower and even negative $\delta^{60}\text{Ni}$ value.

Sorption to minerals can result in fractionation of Ni (e.g. Wasylenki et al., 2015; Ratié et al., 2015). Fe oxides in particular, and also phyllosilicates are scavengers of light Ni. Fractionation due to sorption to these minerals can be observed in weathering profiles (Ratié et al., 2015). In the case of site IR, where chrysotile is the dominant mineral, we do not expect fractionation to be a result of abiotic Ni sorption. At different sites, e.g. BFE, chrysotile and Mg-Fe oxides can be found. However, this mineralogical composition is accompanied by a significantly higher $\delta^{60}\text{Ni}$ than at site IR. Based on this fit between methanogen presence, a low $\delta^{13}\text{C}$ value, and a significantly lower $\delta^{60}\text{Ni}$ value we suggest that the low $\delta^{60}\text{Ni}$ value of site IR may in this case reflect a true biosignature of the present microbial life.

5. Conclusions

- (1) In terrestrial systems, different Ni isotopic compositions prevail. Values typically range between 1 and -1‰. Igneous rocks display values around 0‰, whereas sediments and precipitates deviate more strongly. In the hydrosphere, ocean are generally more Ni enriched and have more constant $\delta^{60}\text{Ni}$ values (+1.21‰ to +1.58‰). Rivers are more depleted in ^{60}Ni and show more variations in $\delta^{60}\text{Ni}$ values between different systems (+0.29‰ to 1.34‰). Rocks display $\delta^{60}\text{Ni}$ values close to 0‰ for igneous rocks, whereas sediments may be strongly fractionated, i.e. strong negative $\delta^{60}\text{Ni}$ values for sulfides (exceeding -1‰) and strong positive $\delta^{60}\text{Ni}$ values for clays and shales (~0.5‰), and nodules (exceeding 1‰).
- (2) Methanogens need Ni for metabolic processes and when absorbing free Ni from the environment prefer lighter Ni, fractionating Ni isotopes between the environment and the cells. When

isotopically analyzing methanogen cell material, this biosignature may be disturbed by the process of cell harvest or by the introduction of organic ligands. The extent of Ni fractionation may be dependent on the concentration of Ni in the environment, i.e. higher Ni concentrations lead to stronger fractionation.

- (3) In addition to biotic fractionation, Ni isotopes can be fractionated abiotically. Sorption of Ni to particles, e.g. phyllosilicates and Fe oxides, fractionates Ni, as lighter Ni is preferentially sorbed to these particles. Ni sorption to organic matter is also shown to produce fractionation patterns similar to metabolic fractionation.
- (4) Fluids from ephemeral fluid seeps on the Tekirova ophiolite exhibit positive $\delta^{60}\text{Ni}$ values and a large variation in $\delta^{60}\text{Ni}$ values. Values range from 1.06 to 1.77‰. Rocks exhibit values closer to one and 5 out of 6 samples are slightly positive, $\sim 0.25\%$. One sample plots distinctly lower at -0.05% . These values agree with normal crustal and riverine values.
- (5) The sample with the lowest $\delta^{60}\text{Ni}$ value coincides with the lowest $\delta^{13}\text{C}$ value. Methanogens are confirmed present here as well. Since the mineralogy does not explain the isotopic anomalies, we suggest that this site may exhibit a true Ni isotopic biosignature. However, we need to distinguish between Ni bearing phases, i.e. the organic matter and the mineral phase.
- (6) The Ni isotope system needs to be better understood before it can be used as a definite biomarker. Ni fractionation in the formation of BIFs is a major issue that should be investigated before we can use Ni isotopes to reveal the relevance of methanogens to the early Earth and the GOE.

6. Martian CH_4 and astrobiology

As mentioned before, CH_4 is not only found on Earth, but on multiple bodies in our solar system, such as our close neighbour Mars (e.g. Webster et al., 2015) or the Saturnian moon of Titan (e.g. Kuiper, 1944; Hanel et al., 1981). The presence of CH_4 and the many ways, both biotic and abiotic, through which it can be produced brings about great interest into the possible systems behind CH_4 cycling on other planets. The fractionation of Ni isotopes by primitive microbes (Cameron et al., 2009; this study) could be a potential biomarker on Earth, but application to extraterrestrial systems is still a very long shot.

The recent planetary exploration of Mars has provided new knowledge of its surface and atmosphere. We now know that CH_4 is present in the Martian atmosphere at about $\sim 10\text{ppb}$ (Mumma et al., 2009). This concentration is low compared to a pre-industrial concentration of $\sim 700\text{ppb}$ and even more so compared to the current concentration of over 1800ppb (NOAA, February 2016) on Earth. Also, lifetime of CH_4 differs greatly, as it is only 10 years on Earth and ~ 300 to ~ 600 years (Atreya et al., 2007) on Mars. The martian atmosphere requires continuous replenishment of CH_4 , but due to the long lifetime and low concentrations, this flux is much smaller than on Earth. To sustain a CH_4 concentration of 10ppb , roughly 126 tonnes of CH_4 must be ejected into the atmosphere per Earth year. This is a very small CH_4 flux when compared to a terrestrial value of 515×10^6 tonnes (Atreya et al., 2007). The origin and source of the Martian CH_4 flux are poorly understood and multiple potential sources have been proposed.

Serpentinization and subsequent Fischer-Tropsch reactions like we encounter on Earth is one of the proposed sources (Etiope et al., 2011b). The presence of basalts and ultramafic rocks on the martian surface (Hoefen et al., 2003; McSween et al., 2004) required for the chemical processes support this theory. Additionally, hydrous alteration minerals, such as serpentine and phyllosilicates have been

found on Mars, implying serpentinizing systems and groundwater flow (Michalski et al., 2013). Such a source can emit CH_4 into the atmosphere through localized seeps as well as dispersed microseepage. An annual emission of 126 tonnes per year requires only a few seeps similar to the ones we find at the Tekirova ophiolite (Etiope et al., 2011b). Ultramafic rocks, like we find at Tekirova, have much higher H_2 yields when serpentinized (McCollom and Bach, 2009). Based on thermodynamic modelling of basalt serpentinization (Wallendahl and Treimann, 1999) it is assumed that the capacity of martian basalts is sufficient to supply atmospheric CH_4 and maintain the low concentrations observed. We would expect that ultramafic rocks, especially when carbonates are present to provide CO_2 , or when gaseous CO_2 is abundant in the martian subsurface (Etiope et al., 2013), will have an even higher CH_4 yield, making serpentinization a likely contributor to martian CH_4 .

While volcanoes on Earth emit large amounts of CH_4 , not even 0.2% of the total CH_4 emissions are a result of volcanic activity (Atreya et al., 2007). This is not a prospective source for Mars as martian volcanoes are no longer active. Besides volcanic inactivity, the SO_2 concentrations of the martian atmosphere do not match a volcanic input of CH_4 . Volcanic gas emissions contain large volumes of SO_2 , and as SO_2 is close to non-existent in the Martian atmosphere (Atreya et al., 2007), a volcanic component of martian CH_4 is highly unlikely.

As comets contain some CH_4 , the observed CH_4 could be residual CH_4 from an old impact. However, this would require an impact with a large ($r = 130$ m) object around 100 years ago or a very large ($r = 360$ m) object within the last 2,000 years (Atreya et al., 2007). Such an event, though improbable, is possible. The concentration of CH_4 can be explained by such a source, but the uneven distribution of CH_4 through the Martian atmosphere makes this a very unlikely contributor.

Another proposed source is slow release of CH_4 from CH_4 clathrate hydrates ($\text{CH}_4 \cdot 6\text{H}_2\text{O}$); crystals of water ice with large spaces accommodating gas molecules. Such structures are capable of compactly storing large amounts of volatiles. Clathrate hydrates on Mars would be stable at depths up to 1km and as shallow as ~ 15 m (Max and Clifford, 2000; Chastain and Chevrier, 2007). The presence of CH_4 trapped in clathrates does not imply any of the possible CH_4 origins. Trapped CH_4 can still be thermogenic, abiogenic or biogenic.

Currently, there is no reason to assume a biotic source to the martian CH_4 cycle. However, a microbial origin of martian CH_4 has not yet been excluded. A subsurface ecosystem, not readily within our reach, may be present. If life were present on Mars, it would likely be as a subsurface ecosystem. The high radiation environment on the surface would make life on it very difficult. In addition, at larger depths, water may be present. With the right geotherm in the martian subsurface, P-T constraints would allow liquid water to be present as shallow as 4km or even shallower in depressed regions (Oze and Sharma, 2005). If water and ambient temperatures are (or were) indeed present at depth, low temperature serpentinization is viable. This in turn, would provide a flux of nutrients in the form of H_2 , trace metals, and heat. It is not known if such a system still exists, but evidence of crustal fluids and groundwater activity suggest that it definitely has in the past and that this may have created environments suitable to a deep subsurface biosphere (Michalski et al., 2013). An important feature of a subsurface ecosystem is its independence. Whereas most ecosystems rely on products of photosynthesis, a subsurface ecosystem may be completely independent and gain all nutrients from a purely mineralogical source. Analogous subsurface ecosystems exist on Earth. Lithoautotrophic microbes, including methanogens, have been found at depths of up to several thousand meters in serpentinizing systems, such as the Columbia River basalt (Stevens and

McKinley, 1995). In the case of the Columbia River basalt lithoautotrophic organisms are found to thrive on serpentinization derived H_2 and could well pose an analogue for life on Mars.

Methanogens studied under pressures applicable to the Martian atmosphere and during freezing and thawing have indicated that some strains of terrestrial methanogens were not hindered by the low pressures or alternating freezing and thawing (Mickol and Kral, 2014). These preliminary results imply that the Martian surface or shallow subsurface may be survivable for terrestrial methanogens.

Future investigation of the Martian CH_4 cycle will shed light on the CH_4 fluxes, the seasonality of CH_4 release into the atmosphere, and subsequently the factors that control CH_4 fluxes. This already will help us understand what controls the martian CH_4 cycle before isotopic data will become available. When isotopic data on CH_4 becomes available we can advance our understanding of martian CH_4 , but as we see on the Tekirova ophiolite, this is not enough. In CH_4 from the Tekirova ophiolite, we cannot observe a biogenic ^{13}C signature, even though we find methanogens and therefore a small biogenic contribution. To properly investigate whether martian CH_4 contains a biogenic component, we must study active CH_4 seeps and other potentially liveable environments. The study of C and H isotopes in CH_4 will also provide a unique insight into the Martian CH_4 cycle and the origin of the gas (Nair et al., 2004)

To be able to determine if life can be present, not only C isotopes should be investigated, but also other traditional and nontraditional isotope systems involved in biotic processes. This includes S for sulphur reducers and oxidizers, Fe for iron reducers and oxidisers, Cu for methanotrophs, and Ni for methanogens. Even then, due to the differences between bulk planetary compositions, interpreting isotope data may be very challenging (Allen et al., 2006). Another major difficulty that has to be overcome is reaching the regions in the crust where life or extinct life could be present or have left its traces, something I deem nearly impossible with the current standards of planetary exploration.

The role of Ni in methanogen life and the preservation of this unique biosignature has to be further investigated before it may be used in the search for terrestrial or extraterrestrial life. Ni can probably not be used on its own, unless we can observe it in microfossils and we can know for sure that the Ni we find is in situ. In other situations, I expect we have to rely on additional isotopes, e.g. C and O, and analysis of organic matter.

Acknowledgements

I would like to thank my supervisors dr. Anna Neubeck and dr. Paul Mason for their feedback and support. I would also like to thank dr. Olivier Rouxel and dr. Emmanuel Ponzevera and the Ifremer Centre de Bretagne. I'm grateful for allowing use of their metal isotope laboratory, MC-ICP-MS facility and the Ni double spike method.

References

1. Albarède, F. & B. Beard. (2004), Analytical Methods for Non-Traditional Isotopes. *Reviews in Mineralogy and Geochemistry* 55(1), pp.113-152.
2. Allen, M., B. Sherwood Lollar, B. Runnegar et al. (2006), Is Mars alive? *Eos, Transactions American Geophysical Union* 87(41), pp.433-439.
3. Anbar, A.D. & O. Rouxel. (2007), Metal Stable Isotopes in Paleoceanography. *Annual Review of Earth and Planetary Sciences* 35(1), pp.717-746.
4. Atreya, S.K., P.R. Mahaffy & A. Wong. (2007), Methane and related trace species on Mars: Origin, loss, implications for life, and habitability. *Planetary and Space Science* 55(3), pp.358-369.
5. Bapteste, É., C. Brochier & Y. Boucher. (2005), Higher-level classification of the Archaea: evolution of methanogenesis and methanogens. *Archaea* 1(5), pp.353-363.
6. Brocks, J.J., G.A. Logan, R. Buick et al. (1999), Archean Molecular Fossils and the Early Rise of Eukaryotes. *Science* 285(5430), pp.1033-1036.
7. Cameron, V. & D. Vance. (2014), Heavy nickel isotope compositions in rivers and the oceans. *Geochimica et Cosmochimica Acta* 128, pp.195-211.
8. Cameron, V., D. Vance, C. Archer et al. (2009), A biomarker based on the stable isotopes of nickel. *Proceedings of the National Academy of Sciences* 106(27), pp.10944-10948.
9. Chastain, B.K. & V. Chevrier. (2007), Methane clathrate hydrates as a potential source for martian atmospheric methane. *Planetary and Space Science* 55(10), pp.1246-1256.
10. Duglokencky, E. (2016). NOAA/ESRL [online]. Retrieved 04/25, 2016. Available on the world wide web: <www.esrl.noaa.gov/gmd/ccgg/trends_ch4/>.
11. Etiope, G., D.Z. Oehler & C.C. Allen. (2011), Methane emissions from Earth's degassing: Implications for Mars. *Planetary and Space Science* 59(2-3), pp.182-195.
12. Etiope, G., M. Schoell & H. Hosgörmez. (2011), Abiotic methane flux from the Chimaera seep and Tekirova ophiolites (Turkey): Understanding gas exhalation from low temperature serpentinization and implications for Mars. *Earth and Planetary Science Letters* 310(1-2), pp.96-104.
13. Etiope, G., B.L. Ehlmann & M. Schoell. (2013), Low temperature production and exhalation of methane from serpentinized rocks on Earth: A potential analog for methane production on Mars. *Icarus* 224(2), pp.276-285.
14. Ferry, J.G. (2010; 2010), How to Make a Living by Exhaling Methane. *Annual Review of Microbiology* 64(1), pp.453-473.
15. Freeman, K.H. & J.M. Hayes. (1992), Fractionation of carbon isotopes by phytoplankton and estimates of ancient CO₂ levels. *Global Biogeochemical Cycles* 6(2), pp.185-198.
16. Fujii, T., F. Moynier, N. Dauphas et al. (2011), Theoretical and experimental investigation of nickel isotopic fractionation in species relevant to modern and ancient oceans. *Geochimica et Cosmochimica Acta* 75(2), pp.469-482.
17. Gall, L., H.M. Williams, C. Siebert et al. (2013), Nickel isotopic compositions of ferromanganese crusts and the constancy of deep ocean inputs and continental weathering effects over the Cenozoic. *Earth and Planetary Science Letters* 375, pp.148-155.
18. Gall, L., H. Williams, C. Siebert et al. (2012), Determination of mass-dependent variations in nickel isotope compositions using double spiking and MC-ICPMS. *Journal of Analytical Atomic Spectrometry* 27(1), pp.137-145.
19. Gramlich, J.W., L.A. Machlan, I.L. Barnes et al. (1989), Absolute Isotopic Abundance Ratios and Atomic Weight of a Reference Sample of Nickel. *Journal of Research of the National Institute of Standards and Technology* 94(6), pp.347-348-356.
20. Gueguen, B., O. Rouxel, E. Ponzevera et al. (2013), Nickel Isotope Variations in Terrestrial Silicate Rocks and Geological Reference Materials Measured by MC-ICP-MS. *Geostandards and Geoanalytical Research* 37(3), pp.297-317.

21. Hanel, R., B. Conrath, F.M. Flasar et al. (1981), Infrared observations of the Saturnian system from voyager 1. *Science* 212(4491), pp.192-200.
22. Hietanen, A.M. (1973), *Geology of the Pulga and Bucks Lake Quadrangles*.
23. Hoefen, T.M., R.N. Clark, J.L. Bandfield et al. (2003), Discovery of Olivine in the Nili Fossae Region of Mars. *Science* 302(5645), pp.627-630.
24. Hösgörmez, H., G. Etiope & M.N. Yalcin. (2008), New evidence for a mixed inorganic and organic origin of the Olympic Chimaera fire (Turkey): a large onshore seepage of abiogenic gas. *Geofluids* 8(4), pp.263-273.
25. Hosgörmez, H. (2007), Origin of the natural gas seep of Çirali (Chimera), Turkey: Site of the first Olympic fire. *Journal of Asian Earth Sciences* 30(1), pp.131-141.
26. Kasting, J.F. (2005), Methane and climate during the Precambrian era. *Precambrian Research* 137(3-4), pp.119-129.
27. Konhauser, K.O., E. Pecoits, S.V. Lalonde et al. (2009), Oceanic nickel depletion and a methanogen famine before the Great Oxidation Event. *Nature* 458(7239), pp.750-753.
28. Konhauser, K.O., L.J. Robbins, E. Pecoits et al. (2015), The Archean Nickel Famine Revisited. *Astrobiology* 15(10), pp.804-815.
29. Kuiper, G.P. (1944), Titan: A satellite with an atmosphere. *Astrophys. J.* 100, pp.378-379-383.
30. Liu, K., S. Kao, K. Chiang et al. (2013), Concentration dependent nitrogen isotope fractionation during ammonium uptake by phytoplankton under an algal bloom condition in the Danshuei estuary, northern Taiwan. *Marine Chemistry* 157, pp.242-252.
31. Max, M.D. & S.M. Clifford. (2000), The state, potential distribution, and biological implications of methane in the Martian crust. *Journal of Geophysical Research: Planets* 105(E2), pp.4165-4171.
32. McCollom, T.M. & W. Bach. (2009), Thermodynamic constraints on hydrogen generation during serpentinization of ultramafic rocks. *Geochimica et Cosmochimica Acta* 73(3), pp.856-875.
33. McSween, H.Y., R.E. Arvidson, J.F. Bell III et al. (2004), Basaltic rocks analyzed by the Spirit rover in Gusev crater. *Science* 305(5685), pp.842-845.
34. Meyer-Dombard, D.R., K.M. Woycheese, E.N. Yargıçoğlu et al. (2015), High pH microbial ecosystems in a newly discovered, ephemeral, serpentinizing fluid seep at Yanartas (Chimera), Turkey. *Frontiers in Microbiology* 6(JAN)
35. Michalski, J.R., J. Cuadros, P.B. Niles et al. (2013), Groundwater activity on Mars and implications for a deep biosphere. *Nature Geosci* 6(2), pp.133-138.
36. Mickol, R.L. & T.A. Kral. (2014), Approaching Martian Conditions: Methanogen Survival at Low Pressure APPROACHING MARTIAN CONDITIONS: METHANOGEN SURVIVAL AT LOW PRES. Conference: Lunar and Planetary Science Conference
37. Millet, M. & N. Dauphas. (2014), Ultra-precise titanium stable isotope measurements by double-spike high resolution MC-ICP-MS. *Journal of Analytical Atomic Spectrometry* 29(8), pp.1444-1458.
38. Moynier, F., J. Blichert-Toft, P. Telouk et al. (2007), Comparative stable isotope geochemistry of Ni, Cu, Zn, and Fe in chondrites and iron meteorites. *Geochimica et Cosmochimica Acta* 71(17), pp.4365-4379.
39. Mumma, M.J., G.L. Villanueva, R.E. Novak et al. (2009), Strong Release of Methane on Mars in Northern Summer 2003. *Science* 323(5917), pp.1041-1045.
40. Nair, H., M.E. Summers, C.E. Miller et al. (2005), Isotopic fractionation of methane in the martian atmosphere. *Icarus* 175(1), pp.32-35.
41. Neubeck, A., D.T. Nguyen & G. Etiope. (2015), Low-temperature dunite hydration: evaluating CH₄ and H₂ production from H₂O and CO₂. *Geofluids*, pp.n/a-n/a.
42. Neubeck, A., Duc, N. T., Bastviken, D. et al. (2011), Formation of H₂ and CH₄ by weathering of olivine at temperatures between 30 and 70°C
<<http://dx.doi.org/10.1186/1467-4866-12-6>>

43. Neubeck, A., N.T. Duc, H. Hellevang et al. (2014), Olivine alteration and H₂ production in carbonate-rich, low temperature aqueous environments. *Planetary and Space Science* 96, pp.51-61.
44. Oze, C. & M. Sharma. (2005), Have olivine, will gas: Serpentinization and the abiogenic production of methane on Mars. *Geophysical Research Letters* 32(10), pp.n/a-n/a.
45. Ragsdale, S.W. (2009), Nickel-based Enzyme Systems. *Journal of Biological Chemistry* 284(28), pp.18571-18575.
46. Ratié, G., D. Jouvin, J. Garnier et al. (2015), Nickel isotope fractionation during tropical weathering of ultramafic rocks. *Chemical Geology* 402, pp.68-76.
47. Rudge, J.F., B.C. Reynolds & B. Bourdon. (2009), The double spike toolbox. *Chemical Geology* 265(3-4), pp.420-431.
48. Schnürer, A., F.P. Houwen & B.H. Svensson. Mesophilic syntrophic acetate oxidation during methane formation by a triculture at high ammonium concentration. *Archives of Microbiology* 162(1), pp.70-74.
49. Seewald, J.S., M.Y. Zolotov & T. McCollom. (2006), Experimental investigation of single carbon compounds under hydrothermal conditions. *Geochimica et Cosmochimica Acta* 70(2), pp.446-460.
50. Siebert, C., T.F. Nägler & J.D. Kramers. (2001), Determination of molybdenum isotope fractionation by double-spike multicollector inductively coupled plasma mass spectrometry. *Geochemistry, Geophysics, Geosystems* 2(7), pp.n/a-n/a.
51. Stevens, T.O. & J.P. McKinley. (1995), Lithoautotrophic Microbial Ecosystems in Deep Basalt Aquifers. *Science* 270(5235), pp.450-455.
52. Thauer, R.K., A. Kaster, M. Goenrich et al. (2010), Hydrogenases from Methanogenic Archaea, Nickel, a Novel Cofactor, and H₂ Storage. *Annual Review of Biochemistry* 79(1), pp.507-536.
53. Wallendahl, A. & A.H. Treiman. (1999). Geochemical models of low-temperature alteration of martian rocks. 30th Annual Lunar and Planetary Science Conference, March 15-29, 1999, Houston, TX,
54. Wasylenki, L.E., H.D. Howe, L.J. Spivak-Birndorf et al. (2015), Ni isotope fractionation during sorption to ferrihydrite: Implications for Ni in banded iron formations. *Chemical Geology* 400, pp.56-64.
55. Watt RK & Ludden PW. Nickel-binding proteins.
56. Webster, C.R., P.R. Mahaffy, S.K. Atreya et al. (2015), Mars methane detection and variability at Gale crater. *Science* 347(6220), pp.415-417.
57. Westerholm, M., S. Roos & A. Schnürer. (2010), *Syntrophaceticus schinkii* gen. nov., sp. nov., an anaerobic, syntrophic acetate-oxidizing bacterium isolated from a mesophilic anaerobic filter. *FEMS microbiology letters* 309(1), pp.100-104.
58. Zehnder, A.J.B., B.A. Huser, T.D. Brock et al. Characterization of an acetate-decarboxylating, non-hydrogen-oxidizing methane bacterium. *Archives of Microbiology* 124(1), pp.1-11.

Appendix A - Reagents and solutions used in Ni elution

1M ammonium citrate

- Ammonium dihydrogen citrate
- 18.2MΩ milli-Q water

CAS: 3012-65-5

Lot No.: A0251867

Acros Organics

Molar mass ammonium citrate: 226.2 g/mol. Amount required for 500ml of solution: 0.5 mol, or 113.1g. 113.1 g was weighed in a balance and added to a 500ml teflon flask. This was then dissolved in 18.2 MΩ milli-q water

0.2M ammonium citrate + NH₄OH

- 1M ammonium nitrate, previously prepared
- concentrated (20-22%) NH₄OH
- 18.2MΩ milli-Q water

CAS (20-22% NH₄OH): 1336-21-6

Lot No.: 7211050

Fisher Chemical

100 ml of 1M ammonium citrate and 400 ml milli-Q 18.2 MΩ water. Tests were performed to find the correct ratio between the 1M amm. citr. and the conc. ammonia to yield pH 9-10.

10ml of 0.2M ammonium citrate was mixed with 0.4 ml of conc. NH₄OH three times, yielding a pH of: 8.4, 9.1, 8.5. Therefore a mixing ratio of 50:2 was adopted and all batches of this solution were prepared with 500ml of 0.2M ammonium citrate and 20ml of concentrated (20-22%) NH₄OH.

Mixing ratio experiment for sample conditioning

Dried samples were prepared by dissolution in 1 ml of 0.24M HCl, 0.3 ml of 1M ammonium citrate and 0.075 ml of concentrated NH₄OH. 4 tests were performed to determine the amount of conc. NH₄OH to be added.

solution	ml	ml	ml	ml
HCl 0.24M	10	10	10	10
Am. Citr. 1M	3	3	3	3
NH ₄ OH 20-22%	1	0.9	0.8	0.75
pH	9.5	9.2	9.0	8.7

However, the volume of conc. NH₄OH was increased to obtain a higher pH, as some samples acidified the columns and hence deactivated the dmg in the Ni-resin. Yields remained very high, even though the pH was >9

Appendix B - Cell culturing and preparation

Methanogens cultured in controlled environments were used here to create sufficiently large amounts of pure methanogen cell material, which could be compared isotopically to the growth medium in order to accurately determine Ni isotope compositions. Cells were cultured at the Department of Microbiology, Swedish University of Agricultural Science, Uppsala.

Cultures consist of 3 pure methanogen strains: the MAB1 strain of methanococcus bourgenis (*MAB1*), Methanosarcina barkeri (*M. barkeri*, DSM 800) and methanobacterium bryantii (*M. bryantii*, DSM 10113). A pure culture of *MAB1* (Schnürer et al., 1994) was provided by the Department of Microbiology, Swedish University of Agricultural Sciences, Uppsala. Samples of *M. barkerii* and *M. bryantii* were provided by the Leibniz Institute DSMZ, the German Collection of Microorganisms and Cell Cultures.

All experiments were conducted in 118 ml borosilicate flasks. To avoid trace metal contamination, all flasks in which cultures were grown, and in addition all rubber seals and disposable plastic instruments were sterilized through a 24h soak in a 20% HCl bath, followed by a 24h soak in a distilled water (Milli-Q 18.2) bath. Bottles were dried overnight at 70°C under perforated plastic film. All culture bottles were sealed with a rubber stop and capped with an aluminium crimp cap. To accurately determine Ni dependence and isotopic fractionation of the different methanogens, the only Ni source in the cultures is the trace metal solution (**E**). Therefore, in the Ni isotope experiment, yeast peptone extract was discarded in order to avoid additional Ni contamination. Absence of yeast extract also decreases the scavenging of light Ni by organic ligands from the yeast peptone extract. Of all 3 provided pure cultures, a 10 ml aliquot was taken and injected into the growth medium using a sterile needle.

Two experiments were performed. The first experiment focused on the influence of Ni availability on the production of CH₄ and the extent of Ni fractionation. Of all three methanogen strains, experiments are set up without added Ni, with the normal medium (as described in Table 1), and with superfluous Ni. During the experiments, the gas composition in the bottles was measured. The second experiment consists of 5 cultures of *MAB1*. Three of the cultures contain no added Ni and two cultures contain the normal growth medium. After several months, some supernatant from a bottle with normal medium was injected into a bottle with normal growth medium. If the methanogens do excrete metabolites, this would be reflected in an increase in CH₄ production in the bottle with injected supernatant, as Ni would be more readily absorbed through metabolite chelation.

Culture media consist of a bicarbonate buffered basal medium prepared from a mixture of multiple different solutions **A** through **I** (Zehnder et al., 1980; modified by Westerholm et al., 2010). First, solutions **A**, **B**, **F** and **I** were mixed in amounts as in **Table 1** and added to 865ml of distilled water, making 1000ml of final solution. This was then boiled to a volume of 0.9L over a period of 20 minutes and cooled while continuously flushed with N₂. Sodium acetate 0.42g L⁻¹ was added to the solution after cooling. The solution was then added to the cultivation flasks and the bottles were sealed with rubber stops, all while flushed with N₂. The bottles were vacuumed and overpressurized with N₂ by 0.2 atm to clear the flasks of all O₂. Vacuuming and overpressurizing was conducted three times and flasks were finally overpressurized by 0.2 atm with N₂/CO₂ (80%:20%). Flasks were autoclaved at 121°C for a period of 20 minutes. Flasks were let to cool and solutions **C1** and **C2** were

injected through a sterile filter (0.2µm) into the flasks using a sterile syringe in amounts as noted in **Table 1**. The final pH of the solution in the flasks was approximately 7.2. The flasks atmospheres were reset using a mixture of H₂/CO₂ with ratio 20%:80% at 1 atm and aliquots of the pure methanogen cultures were added. Culture atmosphere was a mixture of H₂/CO₂ at 20%:80%, which was refilled after 119 days with a fresh 20%:80% mixture of H₂/CO₂. Cells were cultured in the dark at T=37°C and media were not stirred.

Solution	Dissolved species and concentration gL ⁻¹	volume
A ¹	KH ₂ PO ₄ 0.41gL ⁻¹	15 ml
B ¹	Na ₂ HPO ₄ 0.43gL ⁻¹	15 ml
C	NH ₄ Cl 24gL ⁻¹ ; NaCl 24gL ⁻¹ ; CaCl ₂ · 2H ₂ O 8.8gL ⁻¹ ; MgCl ₂ · 6H ₂ O 8gL ⁻¹	12.5 ml (see C1)
C1 ²	E 1 ml; G 1 ml; C 12.5 ml; H ₂ O (Milli-Q 18.2) 34.5 ml	49 ml
C2 ²	D 49ml; H 1 ml; cysteine-HCl 0.5g	50 ml
D (buffer solution)	NaHCO ₃ 80gL ⁻¹	49 ml (see C2)
E (trace metal solution)	FeCl ₂ · 4H ₂ O 2gL ⁻¹ ; H ₃ BO ₃ 0.05gL ⁻¹ ; ZnCl ₂ 0.05gL ⁻¹ ; CuCl ₂ 0.038gL ⁻¹ ; MnCl ₂ · 4H ₂ O 0.41gL ⁻¹ ; (NH ₄) ₆ Mo ₇ O ₂₄ · 4H ₂ O 0.05gL ⁻¹ ; AlCl ₃ 0.05gL ⁻¹ ; CoCl ₂ · 6H ₂ O 0.05gL ⁻¹ ; NiCl ₂ · 6H ₂ O 0.092gL ^{-1*} ; ethylenediaminetetraacetate 0.5gL ⁻¹ ; concentrated HCl 1 ml	1 ml (see C1)
F ¹	Na ₂ SeO ₃ · 5H ₂ O 0.3 gL ⁻¹ ; Na ₂ WO ₄ · 2H ₂ O 0.3 gL ⁻¹	1 ml
G (vitamin solution)	pyridoxamine 0.25 gL ⁻¹ ; nicotinic acid 0.1gL ⁻¹ ; nicotinamide 0.1gL ⁻¹ ; DL-pantothenic acid 0.05gL ⁻¹ ; vitamin B ₁₂ 0.05gL ⁻¹ ; p-aminobenzoic acid 0.05gL ⁻¹ ; pyridoxine hydrochloride 0.1gL ⁻¹ ; biotin 0.02gL ⁻¹ ; thioctic acid 0.05gL ⁻¹ ; folic acid, 0.02gL ⁻¹ ; riboflavin 0.05gL ⁻¹ ; thiamine hydrochloride 0.1gL ⁻¹	1 ml (see C1)
H	Na ₂ S · 9H ₂ O 240.2gL ⁻¹	1 ml (see C2)
I ¹	resazurin 0.5gL ⁻¹	5 ml
H₂O	milli-Q water, 18.2 MΩ	865 ml

Table 1. Solutions used in preparation of the growth medium.

¹ and ² indicate the order of introduction into the growth medium. **C, D, E, G** and **H** were introduced at once in mixtures **C1** and **C2**.

*NiCl · 6H₂O was used instead of NiCl, concentration (gL⁻¹) was adjusted accordingly to yield the same total Ni²⁺ concentration in solution **E**.

To determine the extent of Ni isotope fractionation, both the cell material and the growth medium are analysed. Cells were harvested during the exponential phase of growth by pouring into sterile acid washed falcon tubes. Cultures of the same species were mixed in order to obtain a sufficient

amount of cell material. The medium and cells were separated by centrifugation (Beckman J2-HS centrifuge at 10000 rpm, 15300g) for 20 minutes. During centrifugation, cells concentrated into pellets and after 20 minutes, the supernatant (the cultivation fluid separated from the cell material) was removed and stored as a sample in acid washed falcon tubes. The cells were suspended in a washing liquid (basal medium before addition of C1 and C2) and centrifuged again. This washing procedure was performed twice. After each wash, the washing liquid was removed and stored as a sample. The washed and centrifuged cell pellets dried in falcon tubes at 105°C for 48 hours. There is a total of 12 pellets after mixing of the cultures to be analysed isotopically. Digestion of the cell pellets was performed by adding 5ml of 3M HNO₃ to the falcon tubes, shaking the tubes to suspend as much of the solid material as possible and adding the contents to a teflon vial. Another 5ml of 3M HNO₃ was added to the falcon tubes and the same steps were performed, yielding a total of 10ml of cell material suspension. The teflon vials were placed on a hot plate at 80°C overnight to dissolve as much of the cell material as possible. Since some of the samples did not dissolve fully in acid, they were put on a hot plate and brought to dryness. Samples were then dissolved in concentrated hydrogen peroxide to oxidise and dissolve all organics, freeing all Ni that could have remained trapped in the organics.

Appendix C - Ni elution method

Rocks were dissolved by aqua regia, followed by HF dissolution to fully dissolve all solid remnants. Additionally to a clear solution, precipitates formed in the vials, presumably CaF. As it was impossible to predict if Ni would fractionate by sorption to the precipitates, both the precipitate and clear solution were analysed. Before Ni elution, splits were taken from both the rock solution containing fluoride precipitates (no suffix in **Fig. W**) and the centrifuged clear solution (suffix "(CS)" for centrifuged split in **Fig. W**). This allowed us to test if precipitation of fluorides in the solution affects $\delta^{60}\text{Ni}$ values.

Element concentrations are determined before the Ni elution. Aliquots (<1 ml) were taken from water samples and rock solutions and diluted with 0.28M HNO_3 to a final volume of 10ml. Fe, Ni, Cu and Zn concentrations are measured on an ICP-Quadrupole (ICP-Q-MS, X-series II) at PSO, Brest. Knowing element concentrations allows for optimal spiking of the samples and gives an indication of possible interfering elements. Total Ni content of the sample remainders were calculated.

In preparing the water samples, the contents from the falcon tubes were added to marked teflon beakers and the falcon tubes were rinsed with 2ml of 3M HNO_3 , which was also added to the beakers. Out of 11 samples, 2 fluid samples were found to contain white precipitates. As it is not possible to distinguish between Ni isotopic composition of the precipitate and the fluid, these samples were excluded from further analysis. A specified amount of ^{61}Ni - ^{62}Ni spike is added to each sample (50ppm Ni and 1ppm Ni solution were used to spike precisely). The volume of added spike solution is calculated to yield a $\text{Ni}_{\text{natural}}/\text{Ni}_{\text{spike}}$ ratio of 1. Beakers were placed on a hot plate and the contents brought to dryness. Samples were then prepared for column chromatography. The dry residues are dissolved in 1ml of 0.24M HCl, after which the pH was increased by adding 0.3ml of 1M ammonium citrate and $125\mu\text{l}^1$ of concentrated ammonia (a list of all prepared solutions and used chemicals can be found in Appendix A). Between each addition step 15 minutes were allowed for homogenisation of the solution. Besides samples blanks and NIST SRM 986 standards are prepared. Blanks consist of the same solution that is used to dissolve dry sample residues and a double spike, totalling $10\mu\text{g}$ of Ni.

Columns and their caps were washed by an overnight soak in 10M HCl. Teflon beakers were washed in a 50% HNO_3 bath at 80°C for at least one day. After these acid soaks, columns and beakers were rinsed 3 times with distilled water (Milli-Q 16 M Ω) and left to dry in appropriately cleaned containers.

The chromatography procedure yields samples with very pure Ni and an almost complete absence of contaminants, except insignificantly minor trace amounts of Fe and Cu. This elution step is necessary to prevent interference of Fe and obtain a significantly large signal on all Ni isotopes. To elute Ni, ~3ml columns were loaded with a Ni specific resin (Bio-Rad AG[®] 50W-X8 Resin, 100-200 Mesh). The resin consists of a suspension of microbeads (106–250 μm wet bead size) and water (all mention of water refer to Milli-Q 18.2M Ω distilled water unless otherwise specified). The compound on the microbeads responsible for fixing Ni is dimethylglyoxime, or dmg, which binds to dissolved Ni at pH 9-10 forming a Ni-dmg complex, capturing Ni on the beads. The remaining matrix elements can be rinsed from the column, only to retain Ni. The column setup consists of 24 columns in a

¹ This volume was increased from the predetermined $75\mu\text{l}$ in order to keep the pH high, as some samples lowered the pH due to their acidifying nature.

plexiglass stage under which waste beaker or teflon sample vials can be placed. Each series of samples consisted of 24 samples, including blanks.

0.5 ml of Ni-resin was loaded on the columns. As the required Ni-dmg complex forms at high pH, optimally 9-10, the columns were conditioned to this pH before sample loading. Columns were completely filled (2.2ml) with water 3 times and drained, then filled with a 0.2M ammonium citrate/0.45M ammonia solution twice and drained. After the conditioning the columns were capped and 0.5ml of 0.2M ammonium citrate/0.45M ammonia solution was loaded onto the columns as a buffer solution before sample loading.

The entire prepared sample solution is then loaded onto the columns using a clean pipet and the mixture is then resuspended. Resuspension increases the active surface area of the Ni-resin and therefore the rate of complexation. The suspension is left for 1 hour. During the later MC-ICP-MS procedure, Ni yields were close to 100%, implying the used waiting period of 1 hour is sufficient. After one hour the caps were removed and the columns were let to drain. After draining the columns were filled with 2.2 ml (to full) of the aforementioned solution of 0.2M ammonium citrate + NH_4OH . This step is performed twice, separated by 15 minutes. After this, the columns were loaded with 2.2ml of distilled water, which was performed three times at 15 minutes intervals. After these rinses the matrix elements are washed of.

The contents of the waste beakers are discarded and clean teflon vials are placed under the columns for Ni collection. As the Ni-dmg complex is stable at high pH, acid is used to retrieve the Ni from the complex. To completely break up the Ni-dmg complex, as well as the dmg molecule itself, the columns are filled with 2.2ml of 3M HNO_3 . This step is performed three times at 15 minutes intervals. The retrieved Ni solution is then placed on a hot plate at $\sim 95^\circ\text{C}$ and dried overnight.

The teflon vials are taken from the hot plate, closed and then left to cool down to room temperature. When the beakers have cooled down the dried residue, which is very small in volume, is dissolved for mass spectrometry. 1 ml of 0.28M HNO_3 is added to the residue and the beakers are closed and swirled gently for a few seconds. To samples high in Ni, i.e. dissolved rocks, 2 ml of 0.28M HNO_3 was added. The closed beakers are placed on a hot plate at 80°C for approximately 1 hour to let the HNO_3 vapours cover the entire internal surface area of the beakers and hence fully dissolve the Ni residue. After full dissolution of this residue, the beakers are taken from the hot plate and left to cool down again. When back at room temperature, the beakers were swirled to remove all condensate droplets from the beaker walls and lids and collect all fluid in one volume on the bottom of the beaker. The solution is then transferred to 2ml mass spectrometry vials and analysed on MC-ICP-MS.